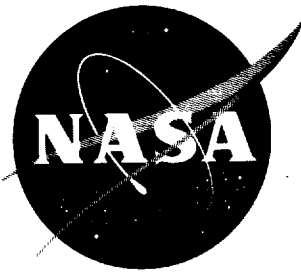


55f

N63-10206  
Code 1  
NASA TN D-1507

NASA TN D-1507



## TECHNICAL NOTE

D-1507

PRESSURE DISTRIBUTION INDUCED ON A FLAT PLATE AT  
A FREE-STREAM MACH NUMBER OF 1.39 BY ROCKETS  
EXHAUSTING UPSTREAM AND DOWNSTREAM

By Abraham Leiss

Langley Research Center  
Langley Station, Hampton, Va.

NATIONAL AERONAUTICS AND SPACE ADMINISTRATION  
WASHINGTON

November 1962



NATIONAL AERONAUTICS AND SPACE ADMINISTRATION

TECHNICAL NOTE D-1507

PRESSURE DISTRIBUTION INDUCED ON A FLAT PLATE AT  
A FREE-STREAM MACH NUMBER OF 1.39 BY ROCKETS  
EXHAUSTING UPSTREAM AND DOWNSTREAM<sup>1</sup>

By Abraham Leiss

SUMMARY

An experimental investigation was made of the pressures induced on a flat plate at a free-stream Mach number of 1.39 by a supersonic rocket jet exhausting upstream and downstream. Measurements of the pressure distribution on a flat plate were made at zero angle of attack for 11 different locations of the jet exhaust nozzle beneath the wing. Measurements were made at ratios of rocket-exit total pressure to free-stream static pressure from 6 to 60 and at a Reynolds number per foot of approximately  $10 \times 10^6$ . The rocket when exhausted upstream produced a strong shock that moved further upstream with increasing rocket-exit total-pressure ratio. Positive incremental normal-force coefficients were obtained at all test positions. Data at 11 test positions are tabulated for rocket-on and rocket-off pressure coefficients as well as for incremental pressure coefficients for the 48 orifices of the flat plate for the range of ratio of rocket-exit total pressure to free-stream static pressure of the investigation. Changing the location of the model with respect to the plate had a negligible effect when the rocket was varied in the chordwise direction, but the pressure coefficients were reduced as the rocket was lowered away from the flat-plate wing.

INTRODUCTION

The Langley Pilotless Aircraft Research Division has been conducting investigations on the effect of propulsive jets on lift, drag, and pressure distributions on flat-plate wings and airplane configurations. The majority of the investigations of this type have been made with jet-exhaust parameters which are characteristic of turbojet engines (for example, refs. 1 to 4). The effects on the flat plate from a rocket jet exhausting perpendicular to the free stream and parallel to the flat plate were

---

<sup>1</sup>Supersedes recently declassified NASA TM X-129 by Abraham Leiss, 1959.

published in reference 5. An initial report on a rocket jet exhausting upstream at a free-stream Mach number of 2.0 beneath a flat surface was presented in reference 6. The present investigation deals with the pressure distributions and loads induced on a flat plate at a free-stream Mach number of 1.39 by rocket jets of design Mach number 3 exhausting upstream and downstream at zero angle of attack for various positions with respect to the plate.

The ratio of rocket total pressure to free-stream static pressure varied from 6 to 60 and the free-stream Reynolds number per foot was approximately  $10 \times 10^6$ . The tests were made in the preflight jet of the NASA Wallops Station.

#### SYMBOLS

A area, sq in.

A,B,...K location of exhaust nozzles or test designations

$\Delta C_N$  incremental normal-force coefficient,  $\frac{F_{N,n} - F_{N,f}}{q_\infty A_T}$

$C_p$  pressure coefficient,  $\frac{p_w - p_\infty}{q_\infty}$

$$\Delta C_p = C_{p,n} - C_{p,f}$$

D diameter, in.

M Mach number

$F_N$  normal force, lb

p static pressure, lb/sq in.

$p_t$  rocket-chamber total pressure, lb/sq in.

$\frac{p_t}{p_\infty}$  rocket-exit total-pressure ratio

q dynamic pressure,  $\frac{\gamma}{2} p_\infty M_\infty^2$ , lb/sq in.

R radius, in.

$\gamma$  specific-heat ratio (for air  $\gamma = 1.4$ ; for rocket mixture  $\gamma = 1.22$ )

x chordwise distance from nacelle exit (positive in direction of rocket jet), in.

y spanwise distance from nacelle center line, in.

Subscripts:

e jet exit

f jet off

n jet on

T nozzle throat

w wing

$\infty$  free stream

#### APPARATUS

The tests were made in the preflight jet facility of the NASA Wallops Station. A 27- by 27-inch nozzle producing a free-stream Mach number of 1.39 was used for these tests. The experimental technique used in this investigation was, first, to mount a flat plate in a free jet blowdown wind tunnel; then a strut-mounted solid-propellant rocket motor was located below the flat surface and ignited during the test. Static pressures on the flat plate were measured to determine the effect of the jet. Photographs of the rocket nacelle mounted in 2 of the 11 test positions beneath the flat plate at the exit of the 27- by 27-inch nozzle are shown as figure 1.

A sketch of the rocket nacelle with its principal dimensions is shown in figure 2. The body of the rocket nacelle had a frontal area of 5.411 square inches with an overall length of 20.9 inches. The exit area  $A_e$  and the throat area  $A_T$  of the convergent-divergent supersonic rocket nozzle were 2.238 and 0.350 square inches, respectively. The exit Mach number  $M_e$  was 3.0 and the value of  $\gamma$  at the exit was 1.22. The rocket nacelle was mounted on a solid hexagonal-shaped support strut. The leading edge of the strut was swept back from the rocket nacelle at

a  $25^{\circ}$  angle and was tapered in plan form from 6 inches at the rocket nacelle to 12 inches at the mounting base 19.5 inches below the rocket nacelle.

Figure 3 shows the location of the rocket nacelle with respect to the wing and preflight-jet nozzle exit for the 11 test positions. The flat plate shown in figure 3 is described in reference 2.

#### INSTRUMENTATION

The rocket-chamber pressure was measured for all of the tests. The location of this pressure orifice is shown in figure 2. The position of 48 static-pressure orifices (0.06-inch inside diameter) on the wing is shown in figure 4. The free-stream total pressure and the stream static pressure were measured 1/2 inch upstream from the exit of the preflight-jet 27- by 27-inch nozzle.

All the pressures were recorded by electrical pressure transducers of the strain-gage type in conjunction with an oscillograph. A 10-cps timer correlated all the time histories. Shadowgraphs, which were made at an exposure of approximately 0.003 second, were obtained by using a carbon-arc light source and a translucent glass screen.

#### TESTS AND METHODS

The lower surface of the wing was rigidly mounted at zero angle of attack 8.3 inches above the center line of the preflight-jet nozzle, which located the wing in the Mach diamond. Tests were made with the rocket nacelle in 11 positions, as shown in figure 3. The vertical plane of the rocket (in every test) was alined with the center line of the flat plate (plane of orifices 1 to 12). At all positions the rocket nacelle was at angles of attack and yaw of  $0^{\circ}$  with respect to both the wing surface and the center line of the preflight jet.

The tests were made by first starting the Mach number 1.39 preflight jet and recording rocket-off data at equilibrium conditions and then firing the rocket and recording rocket-on data. The combustion-chamber pressure varied with the burning of the rocket. The variation of rocket pressure with time was similar during each of the tests. The total firing time of the rocket was approximately 0.6 second. A typical rocket pressure-time curve is presented in figure 5.

## ACCURACY

By allowing for an instrument error of 1 percent of full-scale range, the probable error of the data obtained is believed to be within the following limits:

$C_{p,f}$	.....	.....	±0.02
$C_{p,n}$	.....	.....	±0.02
$p_t/p_\infty$	.....	.....	±0.50
$M_\infty$	.....	.....	±0.02

## RESULTS AND DISCUSSION

### Downstream Firing

Four tests were made with the rocket firing downstream. These tests were made to supplement the data of reference 2. The results are tabulated in tables I to III (tests A, B, C, and D). Table I(a) includes the rocket-off pressure coefficients. Tables II(a) to II(d) present the rocket-on pressure coefficients and tables III(a) to III(d) give the incremental rocket pressure coefficients. Rocket total-pressure ratios up to 60 were obtained by the use of rockets, whereas in reference 2 air jets produced jet total-pressure ratios of only 15.

Figure 6 presents the variation of incremental pressure coefficients, for test position A, with orifice location along the rocket center line for rocket total-pressure ratios of 10, 30, and 50. As in reference 2, the maximum incremental pressure coefficients increased with increased  $p_t/p_\infty$ . Figure 7 shows the effect of vertical distance from the flat plate at a rocket total-pressure ratio of 50. As the rocket exit was moved away from the plate, the initial pressure rises occurred on the plate at a greater distance from the exit. This result conforms with that in appendix A of reference 3.

A comparison with reference 2 at the same exit static-pressure ratios indicated that the magnitude of the induced pressures on the flat plate was about the same even though the exit total-pressure ratios were approximately 10 times greater.

### Upstream Firing

Rocket-off pressure coefficients.- The jet-off pressure coefficients are given in table I(b). Typical jet-off curves are shown in figure 8, which presents the variation of rocket-off pressure coefficient with orifice location for test positions E, F, G, and J. The rocket nacelle in position E has an interference effect on the portion of the plate above the nacelle. As the rocket is lowered, this interference is reduced as indicated by the reduction in positive rocket-off pressure coefficients on the plate for position E to position F (fig. 8) and appears to be non-existent at both positions G and J because the pressure coefficients at these positions are, for all practical purposes, identical. The shadowgraphs in figure 9 illustrate the position of the jet-off shock waves in relation to the flat-plate wing. At test positions E and H the jet-off bow shock intersects the flat plate near the trailing edge. At test position F the bow shock barely intersects the edge of the flat plate and at test positions G, I, J, and K the bow shock misses the flat plate completely.

Rocket-on pressure coefficients.- The experimental jet-on pressure coefficients for individual orifice locations at all test positions for integer values of rocket total-pressure ratio are given in table II. In figure 10 the chordwise variation of jet-on pressure coefficients for test positions E, F, and G is presented at four spanwise positions as a function of distance from the rocket exit  $x/D_T$  at a rocket total-pressure ratio of 46.

The greatest disturbance along the nacelle center line in figure 10(a) occurred at test position E ( $4.985D_T$ ) which was the closest position to the flat plate. This maximum pressure disturbance moved toward the wing trailing edge and was reduced in magnitude as the rocket jet was moved further away from the wing to positions F and G. This effect is not as obvious in the comparison of the different spanwise positions presented in figures 10(b), 10(c), and 10(d). A possible reason for this is the separation of the wing boundary layer. There is some evidence of boundary-layer separation as indicated by the shadowgraphs (fig. 11) because the bow shock splits up into a lambda-leg formation at the intersection with the plate lower surface. Shadowgraphs of the flow field about the rocket exit at various test positions for a jet-on total-pressure ratio of 45 are presented as figure 11. Note that the bow shock, from the jet-off position, has moved upstream to the forward position of the rocket jet exhaust. An explanation of the mixing phenomena is given in reference 6.

Figure 12 presents the variation of rocket-on pressure coefficients with rocket total-pressure ratios for various orifices located on the rocket center line for test position E. Since the higher rocket-exit total-pressure ratio causes the bow shock to move upstream, the jet-on pressure coefficients would be expected to increase and decrease as illustrated in figure 12.

Figure 13 illustrates the chordwise variation of jet-on pressure coefficients with distance from the rocket exit  $x/D_T$  at a rocket total-pressure ratio of 46 for test positions F, I, and J at four spanwise positions. Figure 10 shows the effect of pressure distribution as the rocket is moved vertically away from the plate; figure 13 shows the effect on the pressure distribution as the rocket is moved away parallel to the plate and in the direction of the airstream. The rise in positive pressure begins at approximately the same distance from the rocket exit in figure 13 regardless of the position of the wing trailing edge. This means that the forward penetration of the bow shock is not affected by the wing trailing edge. The reduction in pressure on the wing between position F and position J can probably be attributed to the effects of the variation in wing trailing edge with respect to the rocket exit and its effect upon the local flow conditions on the wing.

#### Incremental Pressure Coefficients

Incremental pressure coefficients  $\Delta C_p$  were obtained by subtracting the jet-off pressure coefficients  $C_{p,f}$  from the jet-on pressure coefficients  $C_{p,n}$ . The incremental pressure coefficients are an indication of the magnitude of the jet effects as obtained from the respective test position. Figure 14 presents the chordwise variation of incremental pressure coefficients at four spanwise stations for test positions E, F, G, I, J, and K at a rocket-exit total-pressure ratio of 46. As shown in the figure, the maximum pressure disturbance due to the bow shock is at about  $7D_T$  to  $9D_T$  away from the rocket exit. Although the values of  $\Delta C_p$  vary, the pressure distributions follow for the different test positions a similar pattern, with the exception of that of test position E. The rocket in test position E is close enough to the flat plate to cause disturbances other than the bow-shock disturbances to the plate. The incremental pressure coefficients for the complete range of rocket-exit total-pressure ratios are presented for all test positions in table III.

#### Normal-Force Coefficients

By using the method of reference 3,  $\Delta C_N$  was obtained by integration and was plotted in figure 15 as a function of rocket-exit total-pressure ratio for test positions F, G, and J. In reference 3, the loads due to the exhausting jet were confined to the area of the plate covered with pressure orifices. The tests described herein were made with the jets exhausting upstream, causing the exhaust effects to cover a larger area than instrumented. The incremental normal-force coefficient is presented as an indication of the normal-force interference only in that part of the interference flow field covered by the plate. Since the greater part of the normal force of test F was past  $x/D_T$  of 11.228, no comparison between test positions of  $\Delta C_N$  can be made. In general,  $\Delta C_N$  increased

as the rocket-exit total-pressure ratio was increased. Positive incremental normal force on the wing was obtained at all test positions.

#### CONCLUSIONS

Experimental studies have been made at a free-stream Mach number of 1.39 with an exit Mach number of 3.0 of a supersonic rocket jet exhausting parallel to a flat-plate surface for exit total-pressure ratios from 6 to 60 in the direction of the free stream and  $180^\circ$  to the free-stream flow. Results of this investigation are summarized as follows:

1. Although the rocket-exit total-pressure ratios of the rocket exhausting downstream were 10 times higher than the jet-exit total-pressure ratios of NACA Research Memorandum L55L13, the pressure coefficients on the flat plate were of the same magnitude when compared at equal jet-exit static-pressure ratios.
2. The maximum pressure coefficients on the flat-plate wing with the rocket exhausting upstream occurred with the rocket exit located at 4.985 rocket throat diameters away from the wing and this maximum value was reduced as the rocket exit was moved further away from the wing.
3. When the rocket exit was varied in the chordwise direction at a constant vertical distance, a negligible change in jet effects occurred.
4. A study of the shadowgraphs of the flat plate shows that the bow shock split into a lambda leg on the lower plate surface, thus indicating separation of the boundary layer in this region.
5. Positive incremental normal force on the wing was obtained at all test positions; the incremental normal force increased with increasing rocket total-pressure ratios.

Langley Research Center,  
National Aeronautics and Space Administration,  
Langley Field, Va., August 27, 1959.

## REFERENCES

1. Bressette, Walter E.: Investigation of the Jet Effects on a Flat Surface Downstream of the Exit of a Simulated Turbojet Nacelle at a Free-Stream Mach Number of 2.02. NACA RM L54E05a, 1954.
2. Bressette, Walter E., and Leiss, Abraham: Investigation of Jet Effects on a Flat Surface Downstream of the Exit of a Simulated Turbojet Nacelle at a Free-Stream Mach Number of 1.39. NACA RM L55L13, 1956.
3. Leiss, Abraham, and Bressette, Walter E.: Pressure Distribution Induced on a Flat Plate by a Supersonic and Sonic Jet Exhaust at a Free-Stream Mach Number of 1.80. NACA RM L56I06, 1957.
4. Bressette, Walter E.: Some Experiments Relating to the Problem of Simulation of Hot Jet Engines in Studies of Jet Effects on Adjacent Surfaces at a Free-Stream Mach Number of 1.80. NACA RM L56E07, 1956.
5. Falanga, Ralph A., and Janos, Joseph J.: Pressure Loads Produced on a Flat-Plate Wing by Rocket Jets Exhausting in a Spanwise Direction Below the Wing and Perpendicular to a Free-Stream Flow of Mach Number 2.0. NASA TN D-893, 1961. (Supersedes NACA RM L58D09.)
6. Bressette, Walter E., and Leiss, Abraham: Effects on Adjacent Surfaces From the Firing of Rocket Jets. NACA RM L57D19a, 1957.

TABLE I.- VALUES OF JET-OFF PRESSURE COEFFICIENTS FOR  
ALL WING ORIFICE POSITIONS

(a) Downstream firing

Orifice ordinates		$C_{p,f}$ at test position -			Orifice ordinates		$C_{p,f}$ at test position
$x/D_T$	$y/D_T$	A	B	C	$x/D_T$	$y/D_T$	D
15.719	0	-0.037	-0.009	-0.016	8.982	0	-0.035
14.596	0	-.019	-.009	-.003	7.859	0	-.023
13.473	0	-.002	-.009	.010	6.737	0	-.055
12.350	0	.014	-.009	-.093	5.614	0	-.077
11.228	0	.038	.038	-.066	4.491	0	-.142
10.105	0	.058	.033	-.051	3.368	0	-.168
8.982	0	.081	-.108	-.019	2.246	0	-.134
7.859	0	.079	-.085	.014	1.123	0	-.067
6.737	0	.046	-.063	.045	0	0	.014
5.614	0	-.054	-.037	.053	-1.123	0	.039
4.491	0	-.165	-.004	.040	-2.246	0	.039
3.368	0	-.173	.017	.042	-3.368	0	.061
15.719	1.497	-.030	-.031	-.001	8.982	1.497	-----
14.596	1.497	-.012	-.014	.007	7.859	1.497	-.030
13.473	1.497	-.003	.006	.004	6.737	1.497	-.026
12.350	1.497	.014	.020	-.088	5.614	1.497	-.072
11.228	1.497	.030	.036	-.074	4.491	1.497	-.082
10.105	1.497	.052	.020	-.058	3.368	1.497	-----
8.982	1.497	.067	-.112	-.025	2.246	1.497	-.164
7.859	1.497	.074	-.080	.012	1.123	1.497	-.118
6.737	1.497	.043	-.061	.050	0	1.497	-.052
5.614	1.497	-.078	-.033	.055	-1.123	1.497	.021
4.491	1.497	-.180	.005	.058	-2.246	1.497	.049
3.368	1.497	-.169	.024	.053	-3.368	1.497	.040
15.719	4.491	.003	-.171	.057	8.982	4.491	-.094
14.596	4.491	.018	.021	.067	7.859	4.491	-.131
13.473	4.491	.013	.019	-.088	6.737	4.491	-.180
12.350	4.491	-.012	.013	-.084	5.614	4.491	-.161
11.228	4.491	.015	-.086	-.087	4.491	4.491	-.140
10.105	4.491	.011	-.136	-.071	3.368	4.491	-.102
8.982	4.491	0	-.114	-.056	2.246	4.491	-.043
7.859	4.491	-.102	-.085	0	1.123	4.491	.014
6.737	4.491	-.148	-.039	.034	0	4.491	.038
5.614	4.491	-.120	.002	.053	-1.123	4.491	.045
4.491	4.491	-.094	.045	.076	-2.246	4.491	.040
15.719	7.485	.020	.023	.045	8.982	7.485	-.155
14.596	7.485	.025	.034	-.067	7.859	7.485	-.150
13.473	7.485	.021	-.012	-.048	6.737	7.485	-.128
12.350	7.485	-.002	.024	-.035	5.614	7.485	-.099
11.228	7.485	-.050	-.021	-.037	4.491	7.485	-.074
10.105	7.485	-.162	-.114	-.054	3.368	7.485	.017
8.982	7.485	-.135	-.090	-.030	2.246	7.485	-.040
7.859	7.485	-.114	-.049	-.004	1.123	7.485	-.006
15.719	11.976	-.140	-.124	-.076	8.982	11.976	-.036
14.596	11.976	-----	-----	-----	7.859	11.976	-----
13.473	11.976	-.117	-.072	-.021	6.737	11.976	-.029
12.350	11.976	-.072	-.051	.001	5.614	11.976	-.035
15.719	14.221	-.125	-.111	-.070	8.982	14.221	-.016

TABLE I-- VALUES OF JET-OFF PRESSURE COEFFICIENTS FOR  
ALL WING ORIFICE POSITIONS - Concluded

(b) Upstream firing

Orifice ordinates		$C_{p,f}$ at test position -			Orifice ordinates		$C_{p,f}$ at test position		Orifice ordinates		$C_{p,f}$ at test position		Orifice ordinates		$C_{p,f}$ at test position -	
$x/D_T$	$y/D_T$	E	F	G	$x/D_T$	$y/D_T$	H	$x/D_T$	$y/D_T$	I	$x/D_T$	$y/D_T$	J	K		
-1.123	0	0.140	0.004	-0.048	-5.614	0	-0.083	2.245	0	-0.045	5.614	0	-0.034	-0.047		
0	0	.209	.002	-.030	-4.491	0	.027	5.368	0	-.050	6.737	0	-.025	-.027		
1.123	0	.125	.004	-.018	-3.368	0	-.032	4.491	0	-.018	7.859	0	-.014	-.021		
2.246	0	-.001	.000	-.009	-2.246	0	.073	5.614	0	-.007	8.982	0	-.011	-.005		
3.368	0	.004	.013	-.007	-1.123	0	.188	6.737	0	0	10.105	0	0	-.001		
4.491	0	-.008	.006	-.017	0	0	.243	7.859	0	-.013	11.228	0	-.009	-.009		
5.614	0	-.003	.009	-.015	1.123	0	.184	8.982	0	-.015	12.350	0	-.001	-.007		
6.737	0	-.014	.002	-.002	2.246	0	.020	10.105	0	-.011	13.473	0	-.003	-.004		
7.859	0	-.006	.004	-.002	3.368	0	-.004	11.228	0	-.008	14.596	0	.001	-.007		
8.982	0	-.007	.004	-.005	4.491	0	-.008	12.350	0	-.009	15.719	0	-.004	-.004		
10.105	0	-.009	.001	.001	5.614	0	-.001	13.473	0	-.007	16.842	0	.004	-.004		
11.228	0	-.005	.003	-.005	6.737	0	-.005	14.596	0	-.006	17.965	0	-.001	0		
-1.123	1.497	.155	.004	----	-5.614	1.497	-.067	2.245	1.497	-.039	5.614	1.497	----	-.041		
0	1.497	.191	.001	-.023	-4.491	1.497	.041	3.368	1.497	-.023	6.737	1.497	-.013	-.024		
1.123	1.497	.106	.013	-.028	-3.368	1.497	-.023	4.491	1.497	-.021	7.859	1.497	-.020	-.015		
2.246	1.497	-.006	.015	-.013	-2.246	1.497	.066	5.614	1.497	-.020	8.982	1.497	-.005	-.019		
3.368	1.497	.001	.002	-.007	-1.123	1.497	.181	6.737	1.497	-.010	10.105	1.497	-.003	-.006		
4.491	1.497	-.008	.003	-.010	0	1.497	.173	7.859	1.497	-.015	11.228	1.497	-.007	-.009		
5.614	1.497	-.007	.009	-.011	1.123	1.497	.106	8.982	1.497	-.016	12.350	1.497	-.007	-.012		
6.737	1.497	.001	.004	-.010	2.246	1.497	.130	10.105	1.497	-.011	13.473	1.497	-.003	-.010		
7.859	1.497	.003	.001	-.005	3.368	1.497	-.010	11.228	1.497	-.009	14.596	1.497	-.003	-.006		
8.982	1.497	-.001	.003	-.006	4.491	1.497	-.013	12.350	1.497	-.011	15.719	1.497	-.001	-.001		
10.105	1.497	-.013	0	-.003	5.614	1.497	-.007	13.473	1.497	-.005	16.842	1.497	-.002	-.001		
11.228	1.497	-.015	0	-.005	6.737	1.497	0	14.596	1.497	-.002	17.965	1.497	-.002	.001		
-1.123	4.491	.113	0	-.059	-5.614	4.491	-.003	2.245	4.491	-.032	5.614	4.491	-.022	-.039		
0	4.491	.116	.003	-.026	-4.491	4.491	-.028	3.368	4.491	-.024	6.737	4.491	-.014	-.029		
1.123	4.491	-.026	.003	-.021	-3.368	4.491	-.037	4.491	4.491	-.022	7.859	4.491	-.014	-.023		
2.246	4.491	-.033	0	-.027	-2.246	4.491	-.109	5.614	4.491	-.022	8.982	4.491	-.015	-.022		
3.368	4.491	-.043	.001	-.079	-1.123	4.491	.143	6.737	4.491	-.037	10.105	4.491	-.030	-.040		
4.491	4.491	-.040	.002	-.004	0	4.491	.130	7.859	4.491	-.041	11.228	4.491	-.037	-.040		
5.614	4.491	-.018	.001	-.023	1.112	4.491	-.014	8.982	4.491	-.021	12.350	4.491	-.020	-.021		
6.737	4.491	-.001	.003	-.006	2.246	4.491	-.004	10.105	4.491	-.009	13.473	4.491	-.003	-.005		
7.859	4.491	.010	.003	.008	3.368	4.491	.004	11.228	4.491	.004	14.596	4.491	.009	.006		
8.982	4.491	.006	.004	.004	4.491	4.491	0	12.350	4.491	-.001	16.842	4.491	.004	.004		
10.105	4.491	.001	-.001	-.003	5.614	4.491	-.002	13.473	4.491	-.002	17.965	4.491	.002	.002		
-1.123	7.485	.052	.003	-.022	-5.614	7.485	-.003	2.245	7.485	-.021	5.614	7.485	-.011	-.027		
0	7.485	-.058	-.001	-.024	-4.491	7.485	.043	3.368	7.485	-.019	6.737	7.485	-.011	-.025		
1.123	7.485	-.044	.002	-.027	-3.368	7.485	.080	4.491	7.485	-.023	7.859	7.485	-.014	-.032		
2.246	7.485	-.053	-.001	-.040	-2.246	7.485	.092	5.614	7.485	-.032	8.982	7.485	-.023	-.042		
3.368	7.485	-.053	.007	-.047	-1.123	7.485	.061	6.737	7.485	-.050	10.105	7.485	-.037	-.051		
4.491	7.485	-.055	.002	-.053	0	7.485	-.061	7.859	7.485	-.053	11.228	7.485	-.046	-.052		
5.614	7.485	-.045	.003	-.058	1.123	7.485	-.045	8.982	7.485	-.040	12.350	7.485	-.032	-.040		
6.737	7.485	-.023	.003	-.018	2.246	7.485	-.023	10.105	7.485	-.016	13.473	7.485	-.009	-.017		
-1.123	11.976	-.057	.002	-.027	-5.614	11.976	.054	2.245	11.976	-.025	5.614	11.976	-.017	-.029		
1.123	11.976	-.037	.002	-.027	-3.368	11.976	.016	4.491	11.976	-.028	7.859	11.976	-.018	-.035		
2.246	11.976	-.059	.001	-.028	-2.246	11.976	-.039	5.614	11.976	-.023	8.982	11.976	-.014	-.026		
3.368	14.221	-.035	.005	-.025	-5.614	14.221	.042	2.245	14.221	-.026	5.614	14.221	-.017	-.031		



TABLE II.- VALUES OF JET-ON PRESSURE COEFFICIENTS FOR WING ORIFICE POSITIONS FOR ROCKET-PRESSURE RATIOS OF 6 TO 60 - Continued

(b) Test position B (downstream firing)

TABLE II.- VALUES OF JET-ON PRESSURE COEFFICIENTS FOR WING CRITICE POSITIONS FOR ROCKET-PRESSURE RATIO OF 6 TO 60 - Continued

POSITIONS FOR HOCKEY-PREPARED HATIOS OF 6 TO 60 - Continued

(c) Test position C (downstream firing)









TABLE II.—VALUES OF JET-ON PRESSURE COEFFICIENTS FOR WING ORIFICE  
POSITIONS FOR FORWARD-PRESSURE RATIO OF 6 TO 60 • Continued

(h) Test Position H (upstream firing)

Orifice ordinates	$x/D_T$	$y/D_T$	Pressure coefficients for forward-pressure ratio $P_1/P_{\infty}$ of -																									
			6	8	10	12	14	16	18	20	22	24	26	28	30	32	34	36	38	40	42	44	46	48	50	52		
-5.614	0	-0.101	-0.109	-0.113	-0.117	-0.121	-0.125	-0.129	-0.133	-0.138	-0.142	-0.146	-0.150	-0.154	-0.158	-0.162	-0.166	-0.170	-0.174	-0.178	-0.182	-0.186	-0.190	-0.194	-0.198			
-4.491	0	-0.047	-0.062	-0.075	-0.084	-0.092	-0.100	-0.104	-0.107	-0.110	-0.115	-0.119	-0.123	-0.127	-0.130	-0.135	-0.139	-0.143	-0.147	-0.151	-0.155	-0.159	-0.163	-0.167	-0.171	-0.175		
-3.368	0	-0.021	-0.029	-0.035	-0.043	-0.051	-0.057	-0.064	-0.071	-0.077	-0.082	-0.088	-0.093	-0.098	-0.102	-0.106	-0.110	-0.114	-0.118	-0.122	-0.126	-0.130	-0.134	-0.138	-0.142	-0.146		
-2.246	0	-0.016	-0.024	-0.031	-0.039	-0.046	-0.053	-0.060	-0.067	-0.074	-0.080	-0.086	-0.092	-0.098	-0.103	-0.108	-0.113	-0.118	-0.123	-0.127	-0.131	-0.135	-0.139	-0.143	-0.147	-0.151		
-1.123	0	-0.010	-0.016	-0.021	-0.026	-0.031	-0.036	-0.041	-0.046	-0.051	-0.056	-0.061	-0.066	-0.071	-0.076	-0.081	-0.086	-0.091	-0.096	-0.101	-0.106	-0.110	-0.114	-0.118	-0.122	-0.126	-0.130	
0	0	-0.007	-0.013	-0.019	-0.024	-0.029	-0.034	-0.039	-0.044	-0.049	-0.054	-0.059	-0.064	-0.069	-0.074	-0.079	-0.084	-0.089	-0.094	-0.099	-0.104	-0.109	-0.113	-0.117	-0.121	-0.125	-0.129	
1.123	0	-0.017	-0.027	-0.033	-0.039	-0.045	-0.051	-0.057	-0.063	-0.069	-0.075	-0.081	-0.087	-0.093	-0.098	-0.104	-0.109	-0.115	-0.120	-0.125	-0.130	-0.135	-0.140	-0.145	-0.150	-0.155	-0.160	
2.346	0	-0.016	-0.025	-0.033	-0.041	-0.049	-0.056	-0.063	-0.070	-0.077	-0.084	-0.091	-0.098	-0.105	-0.112	-0.119	-0.125	-0.131	-0.137	-0.143	-0.149	-0.155	-0.161	-0.167	-0.173	-0.179	-0.185	
3.368	0	-0.008	-0.013	-0.017	-0.023	-0.027	-0.033	-0.039	-0.044	-0.049	-0.055	-0.061	-0.066	-0.071	-0.076	-0.081	-0.086	-0.091	-0.096	-0.101	-0.106	-0.111	-0.116	-0.121	-0.126	-0.131	-0.136	
4.491	0	-0.005	-0.009	-0.013	-0.017	-0.021	-0.025	-0.029	-0.033	-0.037	-0.041	-0.046	-0.050	-0.055	-0.059	-0.064	-0.068	-0.073	-0.077	-0.081	-0.086	-0.090	-0.094	-0.098	-0.102	-0.106	-0.110	
5.614	0	-0.003	-0.006	-0.009	-0.012	-0.015	-0.018	-0.021	-0.024	-0.027	-0.030	-0.034	-0.037	-0.041	-0.045	-0.049	-0.053	-0.057	-0.061	-0.065	-0.069	-0.073	-0.077	-0.081	-0.085	-0.089	-0.093	
6.737	0	-0.007	-0.012	-0.016	-0.021	-0.026	-0.030	-0.035	-0.039	-0.043	-0.047	-0.051	-0.055	-0.059	-0.063	-0.067	-0.071	-0.075	-0.079	-0.083	-0.087	-0.091	-0.095	-0.099	-0.103	-0.107	-0.111	
-5.614	1.497	-0.090	-0.095	-0.100	-0.105	-0.110	-0.115	-0.119	-0.123	-0.127	-0.131	-0.135	-0.139	-0.143	-0.147	-0.151	-0.155	-0.159	-0.163	-0.167	-0.171	-0.175	-0.179	-0.183	-0.187	-0.191	-0.195	
-4.491	1.497	-0.095	-0.099	-0.103	-0.107	-0.111	-0.115	-0.119	-0.123	-0.127	-0.131	-0.135	-0.139	-0.143	-0.147	-0.151	-0.155	-0.159	-0.163	-0.167	-0.171	-0.175	-0.179	-0.183	-0.187	-0.191	-0.195	
-3.368	1.497	-0.086	-0.090	-0.094	-0.098	-0.102	-0.106	-0.110	-0.114	-0.118	-0.122	-0.126	-0.130	-0.134	-0.138	-0.142	-0.146	-0.150	-0.154	-0.158	-0.162	-0.166	-0.170	-0.174	-0.178	-0.182	-0.186	
-2.346	1.497	-0.075	-0.080	-0.084	-0.088	-0.092	-0.096	-0.100	-0.104	-0.108	-0.112	-0.116	-0.120	-0.124	-0.128	-0.132	-0.136	-0.140	-0.144	-0.148	-0.152	-0.156	-0.160	-0.164	-0.168	-0.172	-0.176	
-1.123	1.497	-0.065	-0.071	-0.075	-0.080	-0.084	-0.088	-0.092	-0.096	-0.100	-0.104	-0.108	-0.112	-0.116	-0.120	-0.124	-0.128	-0.132	-0.136	-0.140	-0.144	-0.148	-0.152	-0.156	-0.160	-0.164	-0.168	
0	1.497	-0.055	-0.060	-0.064	-0.068	-0.072	-0.076	-0.080	-0.084	-0.088	-0.092	-0.096	-0.100	-0.104	-0.108	-0.112	-0.116	-0.120	-0.124	-0.128	-0.132	-0.136	-0.140	-0.144	-0.148	-0.152	-0.156	
1.123	1.497	-0.045	-0.050	-0.055	-0.059	-0.063	-0.067	-0.071	-0.075	-0.079	-0.083	-0.087	-0.091	-0.095	-0.099	-0.103	-0.107	-0.111	-0.115	-0.119	-0.123	-0.127	-0.131	-0.135	-0.139	-0.143	-0.147	
2.346	1.497	-0.035	-0.039	-0.043	-0.047	-0.051	-0.055	-0.059	-0.063	-0.067	-0.071	-0.075	-0.079	-0.083	-0.087	-0.091	-0.095	-0.099	-0.103	-0.107	-0.111	-0.115	-0.119	-0.123	-0.127	-0.131	-0.135	
3.368	1.497	-0.025	-0.029	-0.033	-0.037	-0.041	-0.045	-0.049	-0.053	-0.057	-0.061	-0.065	-0.069	-0.073	-0.077	-0.081	-0.085	-0.089	-0.093	-0.097	-0.101	-0.105	-0.109	-0.113	-0.117	-0.121	-0.125	
4.491	1.497	-0.015	-0.019	-0.023	-0.027	-0.031	-0.035	-0.039	-0.043	-0.047	-0.051	-0.055	-0.059	-0.063	-0.067	-0.071	-0.075	-0.079	-0.083	-0.087	-0.091	-0.095	-0.099	-0.103	-0.107	-0.111	-0.115	
5.614	1.497	-0.005	-0.008	-0.011	-0.014	-0.017	-0.020	-0.024	-0.027	-0.030	-0.034	-0.037	-0.041	-0.045	-0.049	-0.053	-0.057	-0.061	-0.065	-0.069	-0.073	-0.077	-0.081	-0.085	-0.089	-0.093	-0.097	-0.101
6.737	1.497	-0.002	-0.004	-0.006	-0.008	-0.010	-0.012	-0.014	-0.016	-0.018	-0.020	-0.023	-0.025	-0.028	-0.030	-0.033	-0.035	-0.038	-0.040	-0.042	-0.045	-0.048	-0.051	-0.054	-0.057	-0.060	-0.063	
-5.614	4.491	-0.065	-0.077	-0.089	-0.099	-0.109	-0.119	-0.128	-0.137	-0.146	-0.154	-0.162	-0.170	-0.178	-0.186	-0.194	-0.202	-0.210	-0.218	-0.226	-0.234	-0.242	-0.250	-0.258	-0.266	-0.274	-0.282	-0.290
-4.491	4.491	-0.053	-0.061	-0.069	-0.075	-0.081	-0.087	-0.093	-0.099	-0.104	-0.110	-0.116	-0.122	-0.128	-0.134	-0.140	-0.146	-0.152	-0.158	-0.164	-0.170	-0.176	-0.182	-0.188	-0.194	-0.200	-0.206	
-3.368	4.491	-0.040	-0.049	-0.056	-0.063	-0.070	-0.076	-0.083	-0.089	-0.095	-0.101	-0.107	-0.113	-0.119	-0.125	-0.131	-0.137	-0.143	-0.149	-0.155	-0.161	-0.167	-0.173	-0.179	-0.185	-0.191	-0.197	
-2.346	4.491	-0.028	-0.034	-0.040	-0.046	-0.051	-0.057	-0.063	-0.068	-0.073	-0.078	-0.083	-0.088	-0.093	-0.098	-0.103	-0.108	-0.113	-0.118	-0.123	-0.128	-0.133	-0.138	-0.143	-0.148	-0.153	-0.158	-0.163
-1.123	4.491	-0.017	-0.023	-0.028	-0.033	-0.038	-0.043	-0.048	-0.053	-0.058	-0.063	-0.068	-0.073	-0.078	-0.083	-0.088	-0.093	-0.098	-0.103	-0.108	-0.113	-0.118	-0.123	-0.128	-0.133	-0.138	-0.143	
0	4.491	-0.005	-0.009	-0.013	-0.017	-0.021	-0.025	-0.029	-0.033	-0.037	-0.041	-0.045	-0.049	-0.053	-0.057	-0.061	-0.065	-0.069	-0.073	-0.077	-0.081	-0.085	-0.089	-0.093	-0.097	-0.101	-0.105	
1.123	4.491	-0.002	-0.004	-0.006	-0.008	-0.010	-0.012	-0.014	-0.016	-0.018	-0.020	-0.022	-0.024	-0.026	-0.028	-0.030	-0.032	-0.034	-0.036	-0.038	-0.040	-0.042	-0.044	-0.046	-0.048	-0.050	-0.052	
2.346	4.491	-0.001	-0.002	-0.003	-0.004	-0.005	-0.006	-0.007	-0.008	-0.009	-0.010	-0.011	-0.012	-0.013	-0.014	-0.015	-0.016	-0.017	-0.018	-0.019	-0.020	-0.021	-0.022	-0.023	-0.024	-0.025	-0.026	
3.368	4.491	-0.000	-0.001	-0.002	-0.003	-0.004	-0.005	-0.006	-0.007	-0.008	-0.009	-0.010	-0.011	-0.012	-0.013	-0.014	-0.015	-0.016	-0.017	-0.018	-0.019	-0.020	-0.021	-0.022	-0.023	-0.024	-0.025	
-1.123	7.485	-0.069	-0.084	-0.098	-0.109	-0.121	-0.132	-0.143	-0.153	-0.164	-0.174	-0.184	-0.194	-0.204	-0.214	-0.224	-0.234	-0.244	-0.254	-0.264	-0.274	-0.284	-0.294	-0.304	-0.314	-0.324	-0.334	-0.344
0	7.485	-0.056	-0.065	-0.075	-0.084	-0.093	-0.102	-0.111	-0.120	-0.129	-0.138	-0.147	-0.156	-0.165	-0.174	-0.183	-0.192	-0.201	-0.210	-0.219	-0.228	-0.237	-0.246	-0.255	-0.264	-0.273	-0.282	-0.291
1.123	7.485	-0.045	-0.051	-0.057	-0.064	-0.071	-0.078	-0.085	-0.092	-0.099	-0.106	-0.113	-0.120	-0.127	-0.134	-0.141	-0.148	-0.155	-0.162	-0.169	-0.176	-0.183	-0.190	-0.197	-0.204	-0.211	-0.218	-0.225
2.346	7.485	-0.035	-0.040	-0.046	-0.051	-0.057	-0.063	-0.068	-																			





TABLE II.—VALUES OF JET-ON PRESSURE COEFFICIENTS FOR WING ORIFICE

COLLISIONS FOR ROCKE-1 PHOTON RADIUS OF  $R_A = 1.61 \pm 0.01$

(k) Test position K (upstream firing)













TABLE III.—VALUES OF INCREMENTAL PRESSURE COEFFICIENTS FOR TING ORIFICE POSITIONS FOR ROCKET-PRESSURE RATIOS OF 6 TO 50. —Continued

OPTIMIZATIONS FOR ROCKET-PRESSURE RATIOS OF 6 TO 30 : CONTINUED

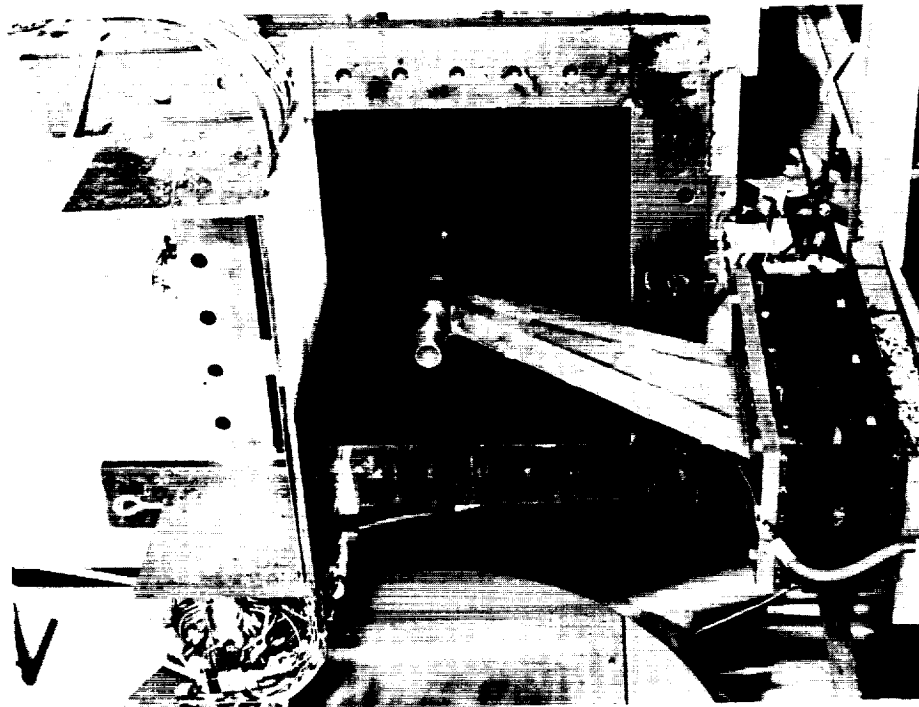
(g) Test position 6 (unstressed string)



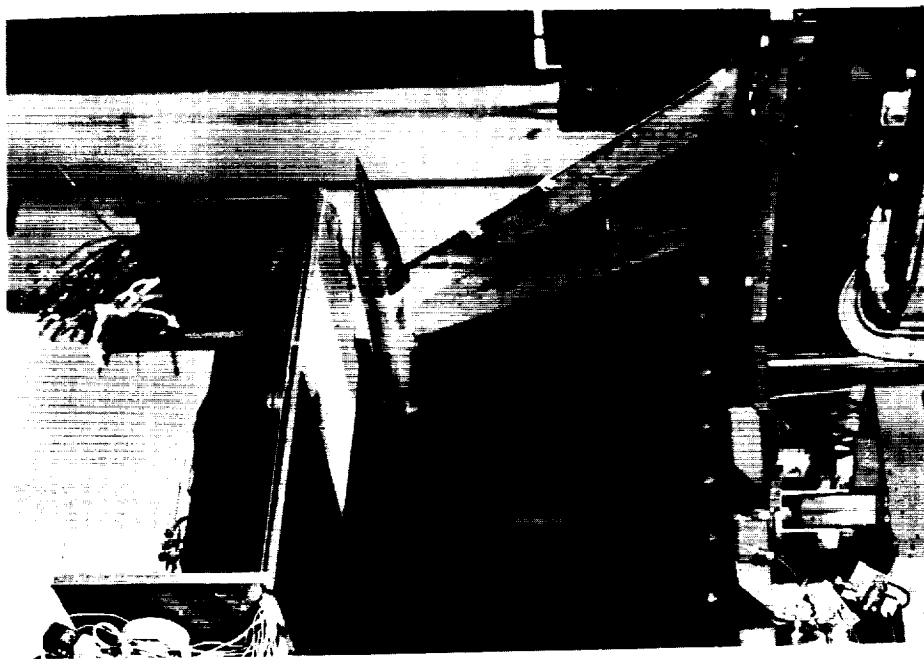








(a) Downstream firing. L-57-373



(b) Upstream firing. L-57-231

Figure 1.- Rocket mounted in two test positions beneath the flat-surface wing attached to the 27- by 27-inch preflight-jet nozzle.

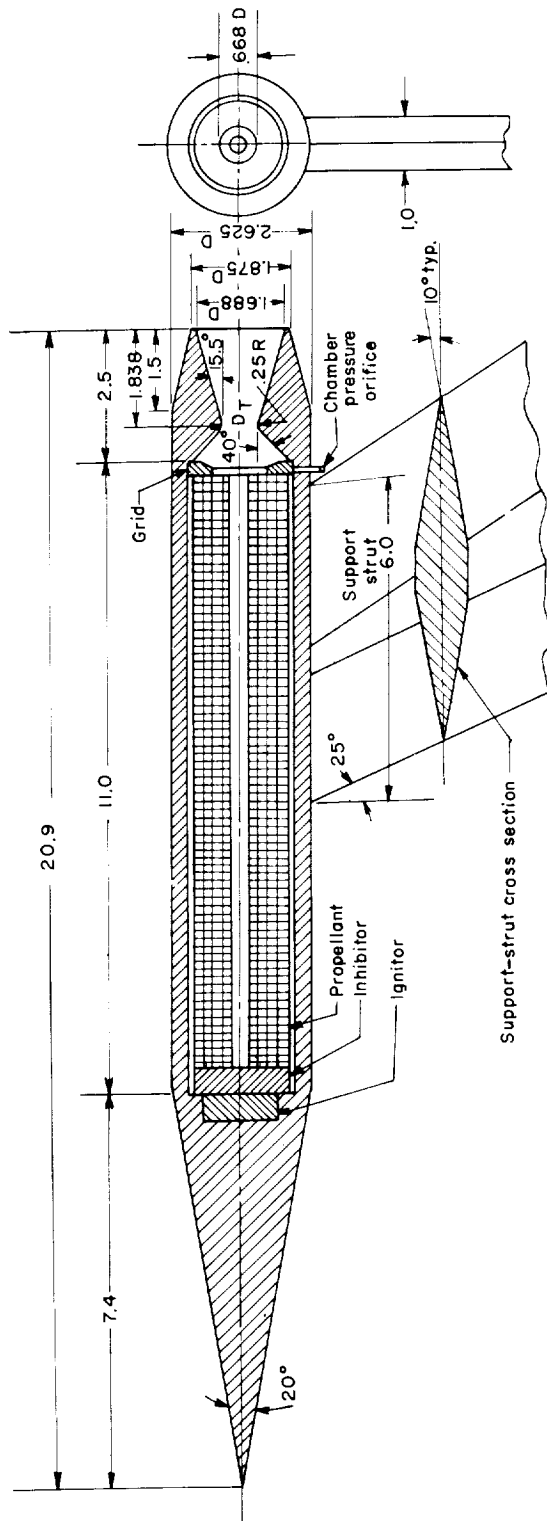


Figure 2.- Schematic sketch of rocket nacelle. All dimensions are in inches except as otherwise noted.

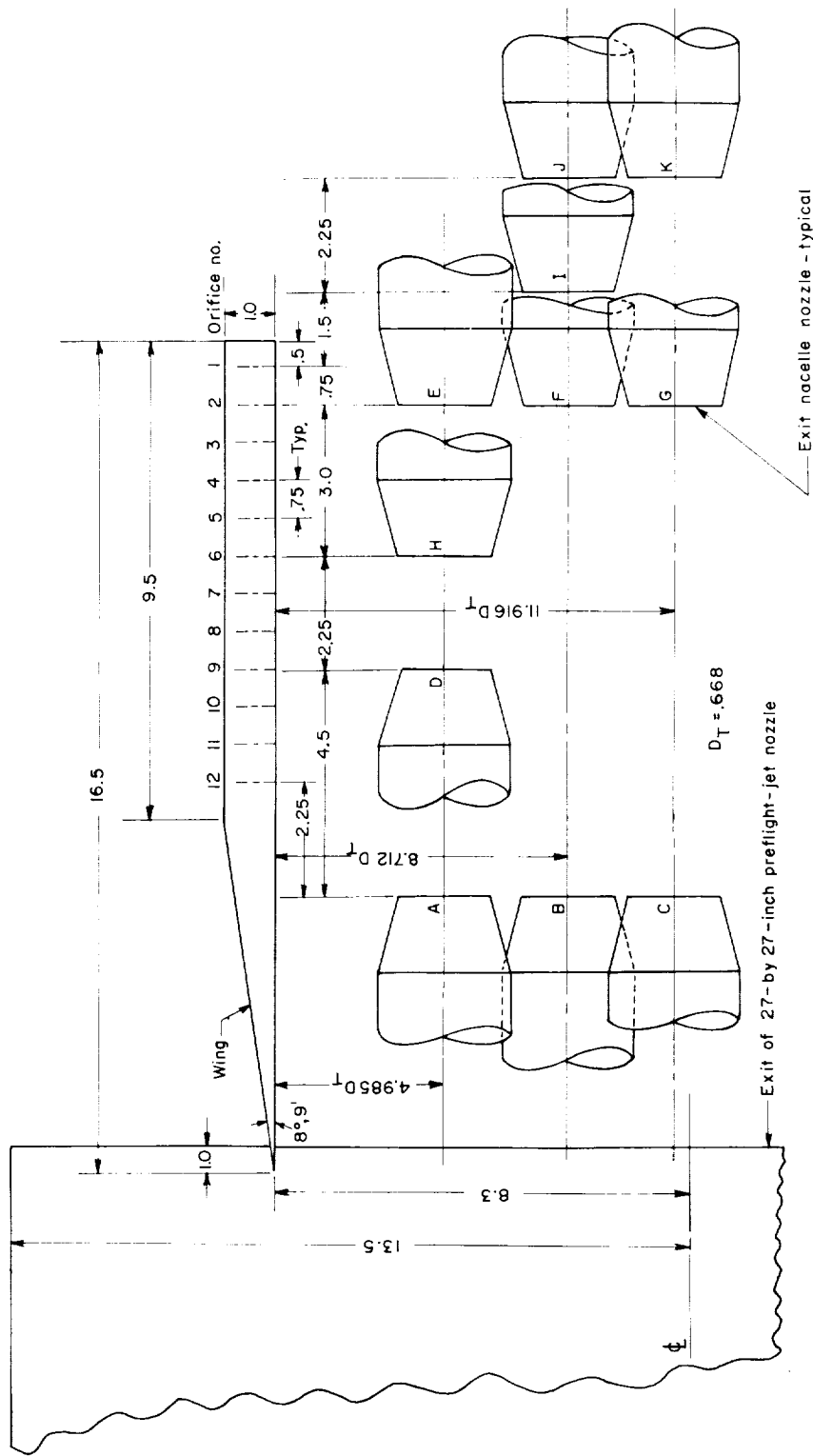


Figure 3.- Arrangement of the rocket nacelle relative to the exit of the 27- by 27-inch preflight-jet nozzle and wing for the eleven test positions. Dimensions are in inches except as otherwise noted.

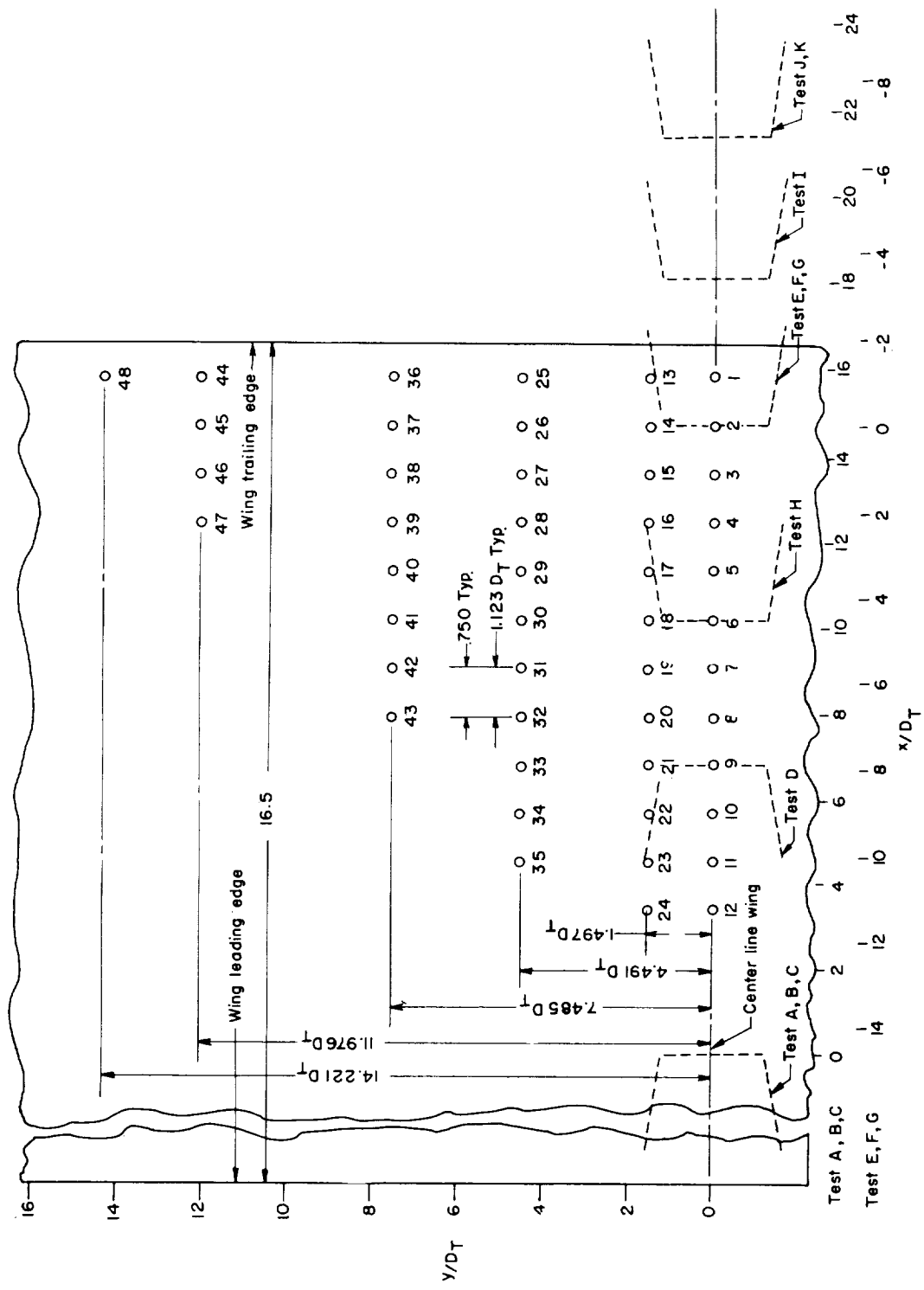


Figure 4.- Locations of the 48 wing static-pressure orifices and orifice designations as well as rocket nacelle location for each test. All dimensions are in inches unless otherwise noted.

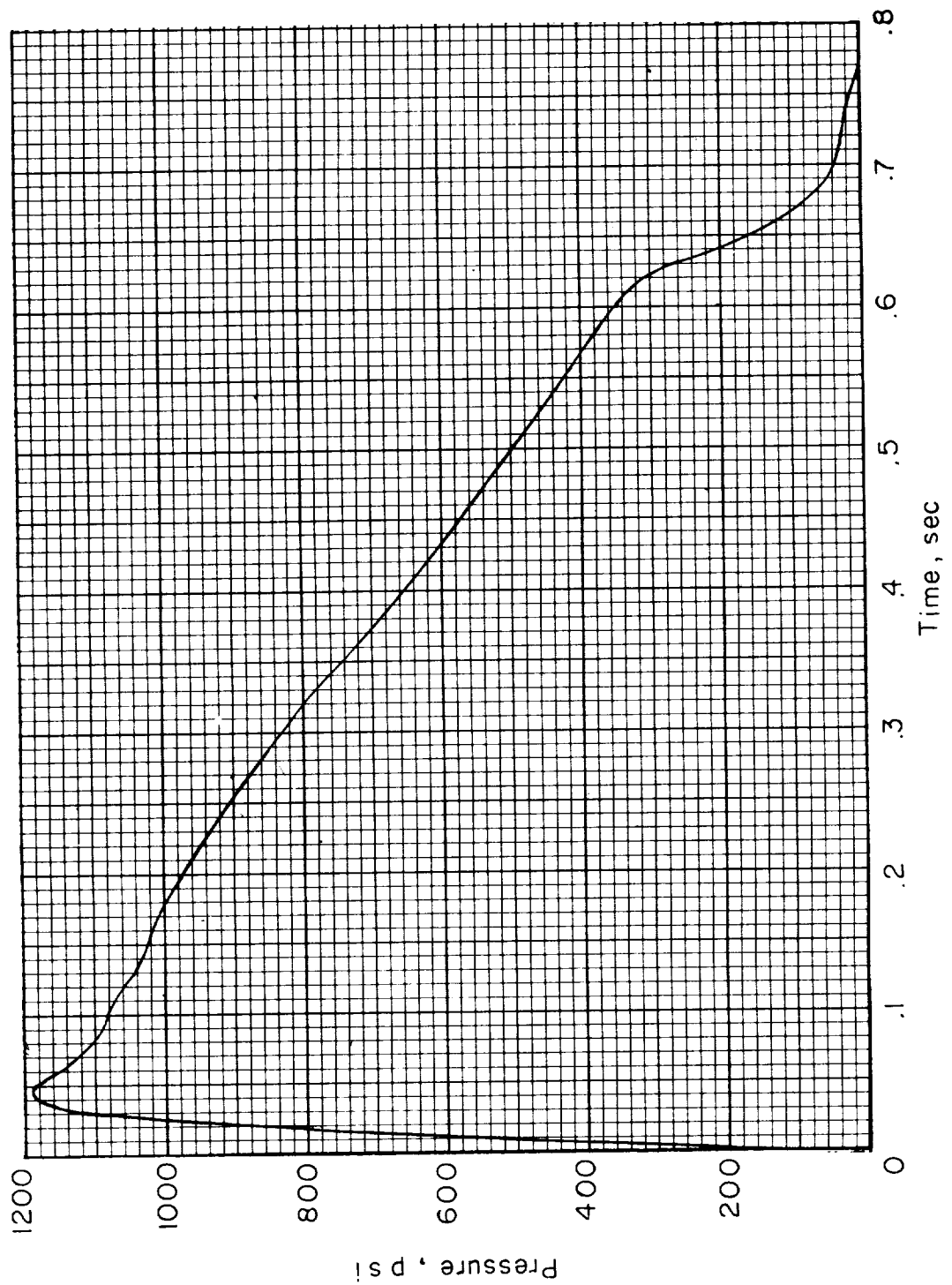


Figure 5.- Typical variation of rocket pressure with time.

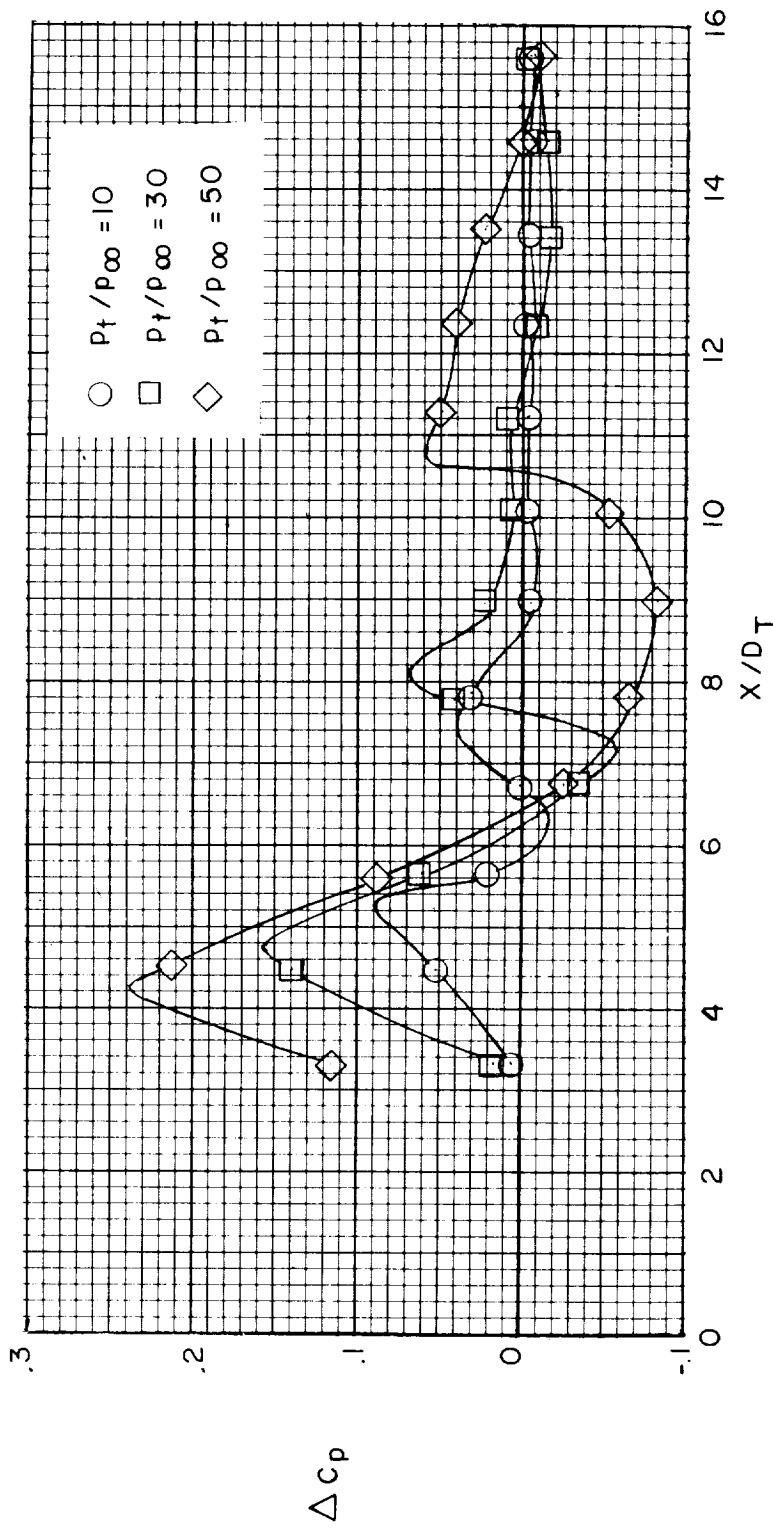


Figure 6.- Variation of incremental pressure coefficients for test position A with orifice location along the rocket center line for rocket pressure ratios of 10, 30, and 50.

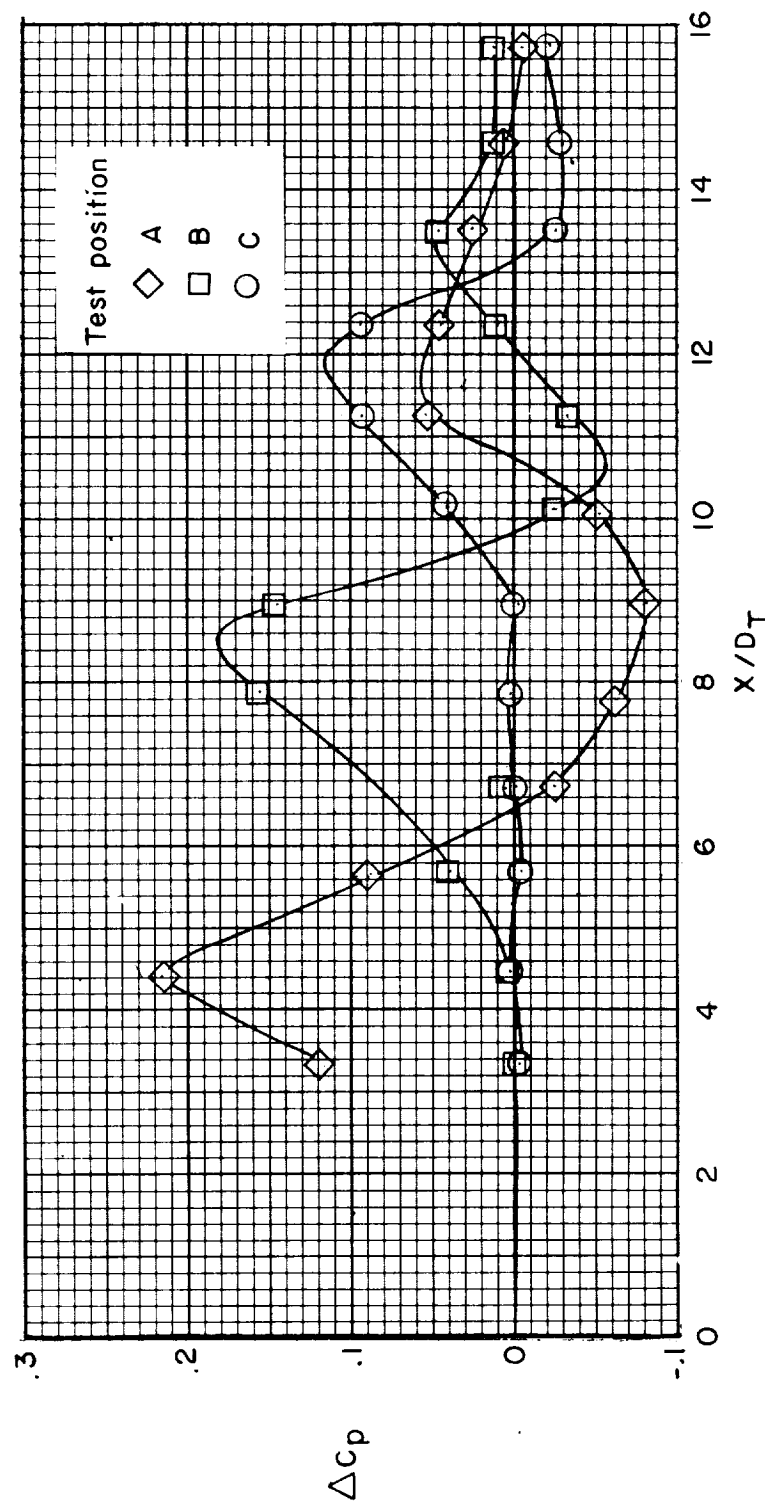


Figure 7.- Variation of incremental pressure coefficients for rocket pressure ratio of 50 along the rocket center line for test positions A, B, and C.

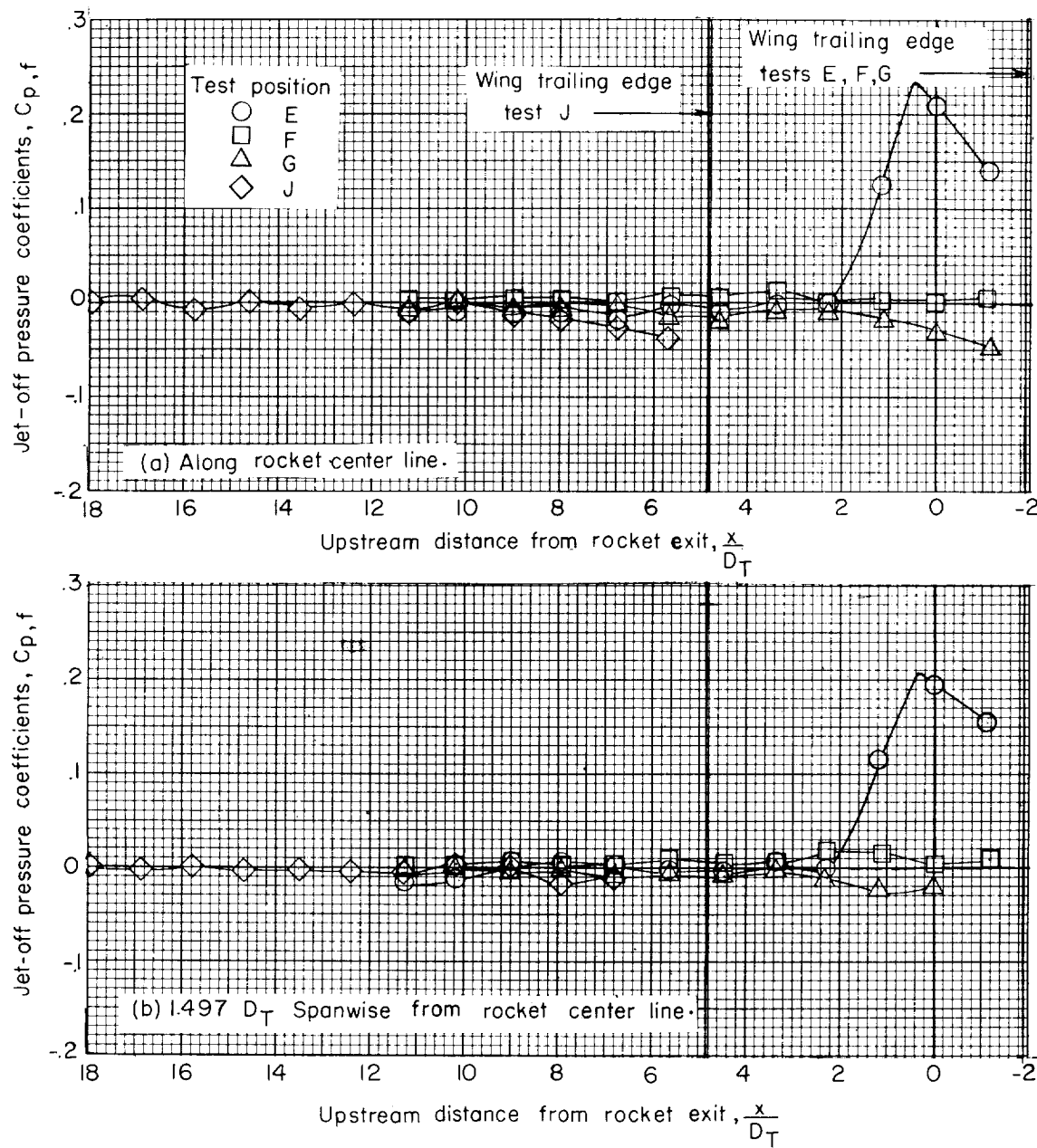


Figure 8.- Chordwise variation of jet-off pressure coefficients for test positions E, F, G, and J.

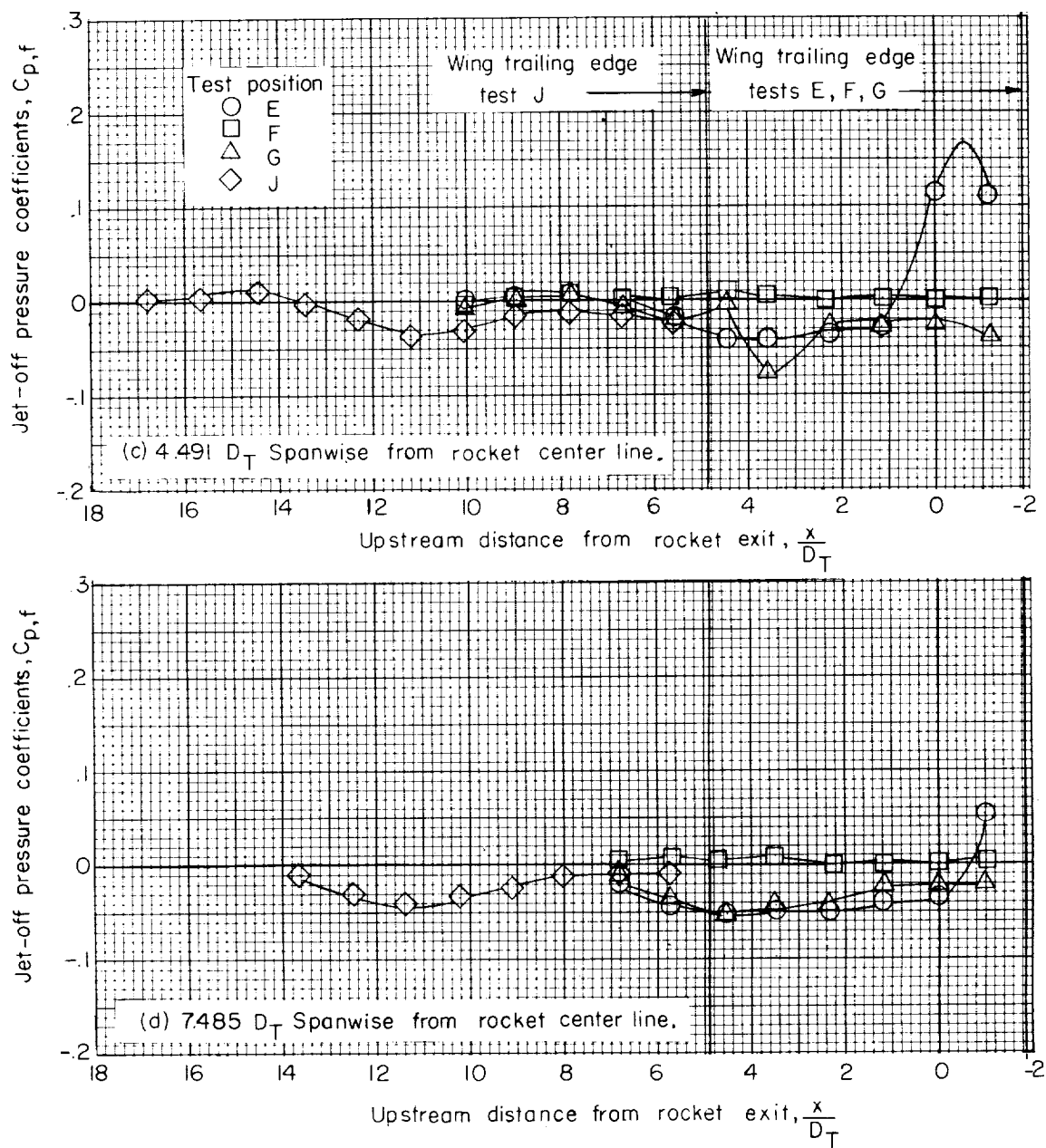
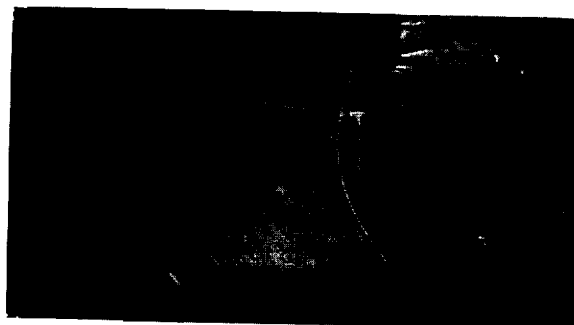
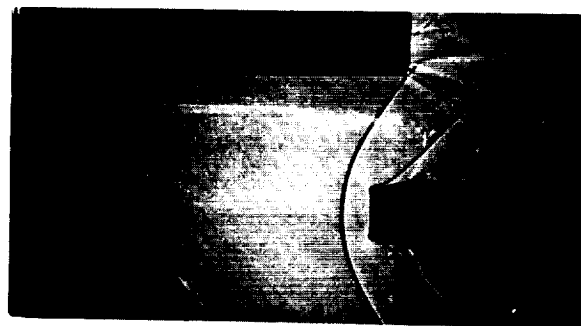


Figure 8.- Concluded.



Test position E



Test position F

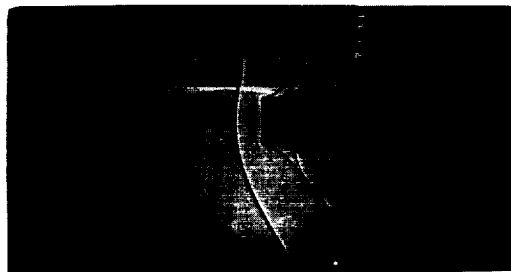


Test position G

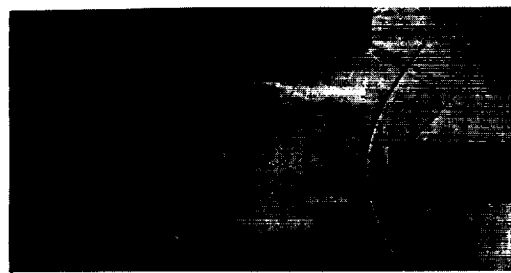
(a) Test positions E, F, and G.

L-59-6016

Figure 9.- Shadowgraphs of the flow field about the rocket exit with jet off for test positions E, F, G, H, I, J, and K.



Test position H



Test position I



Test position J



Test position K

(b) Test positions H, I, J, and K.

L-59-6017

Figure 9.- Concluded.

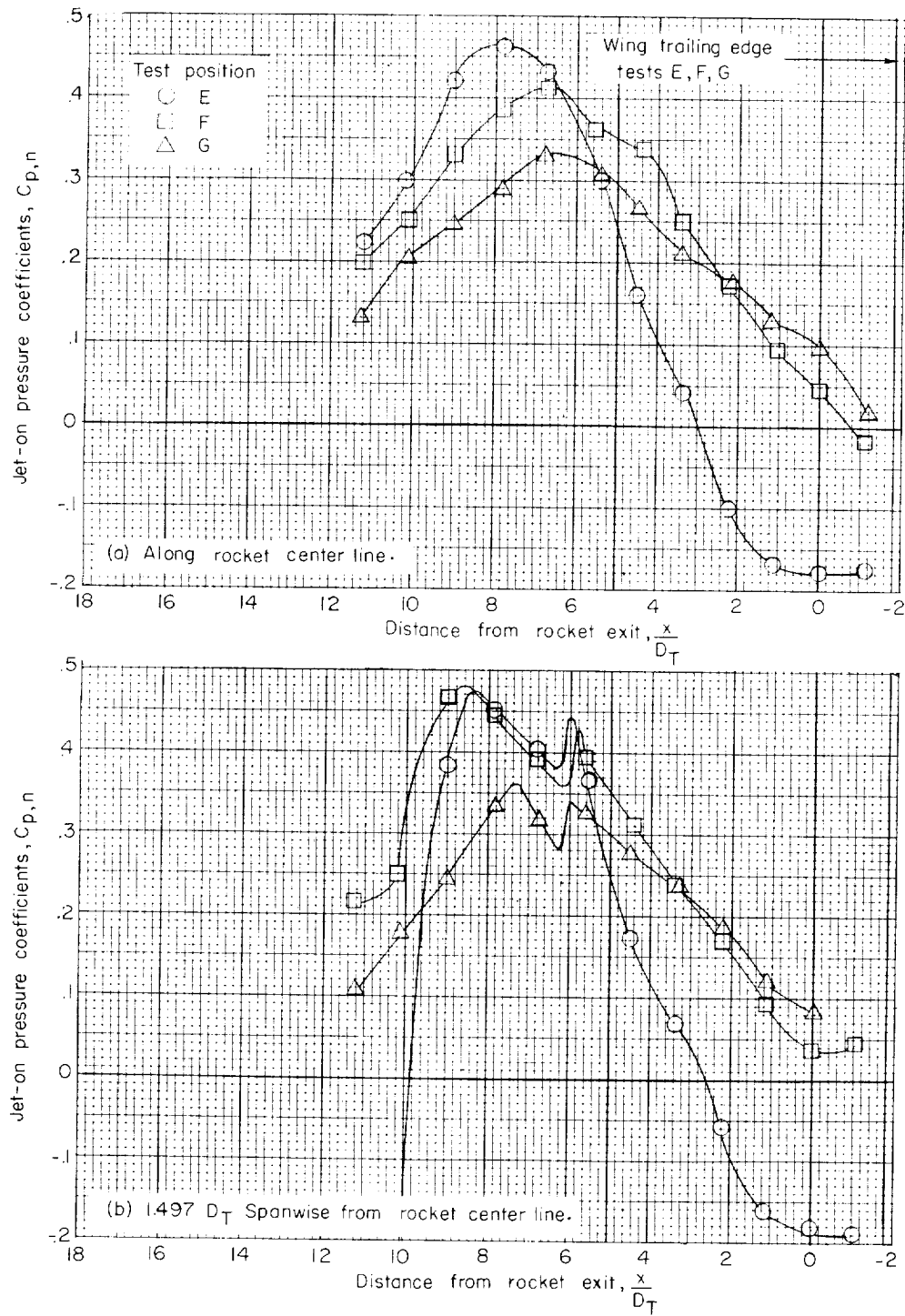


Figure 10.- Chordwise variation of jet-on pressure coefficients at positions E, F, and G for a rocket pressure ratio of 46.

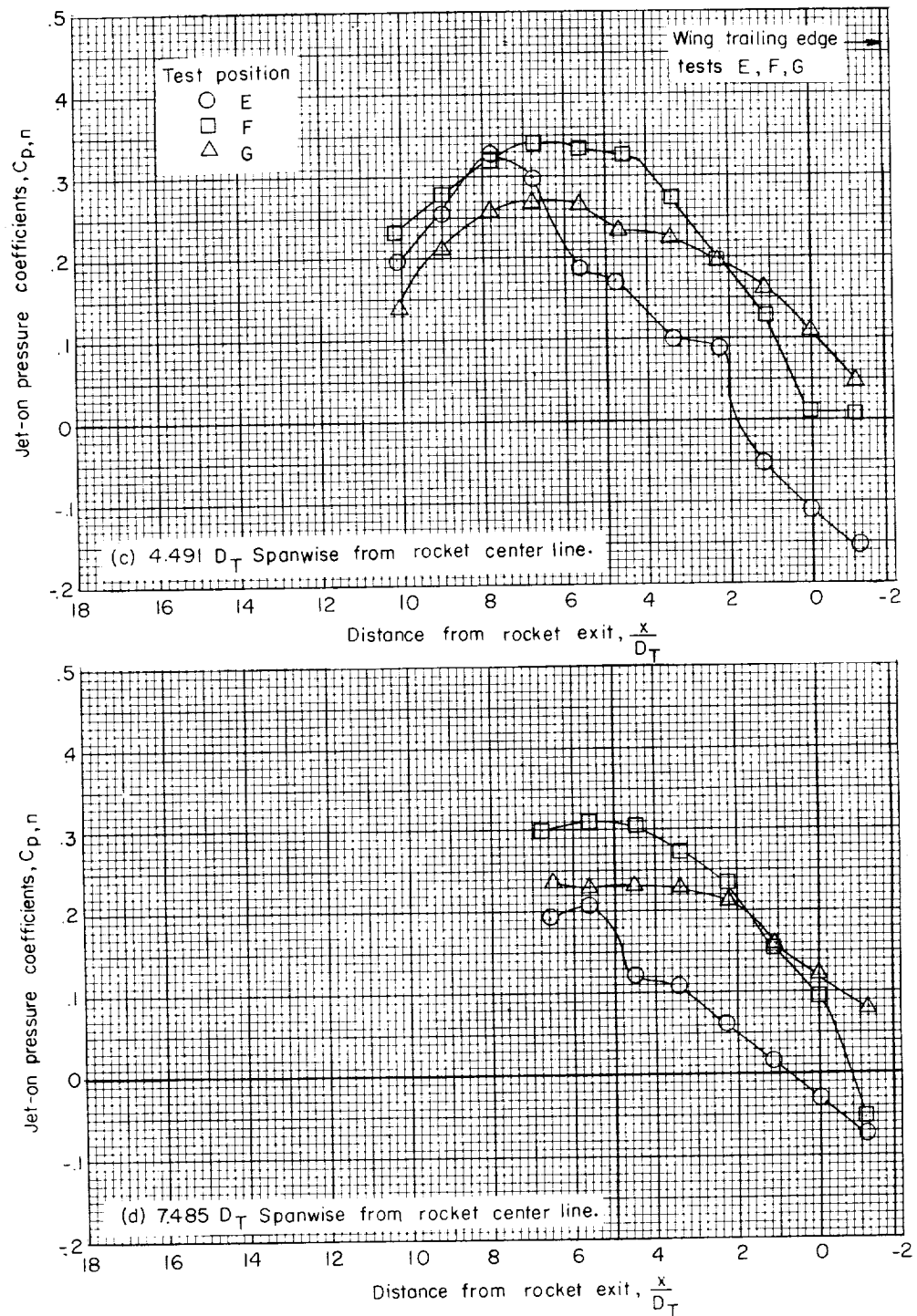


Figure 10.- Concluded.



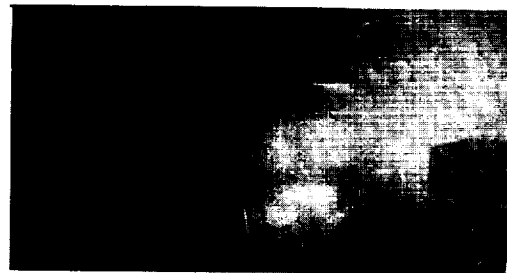
(a) Test position E.



(d) Test position I.



(b) Test position F.



(e) Test position J.



(c) Test position G.

(f) Test position K.  
L-59-5100

Figure 11.- Shadowgraphs of the flow field about the rocket exit for a total-pressure ratio of 45 at test positions E, F, G, I, J, and K.

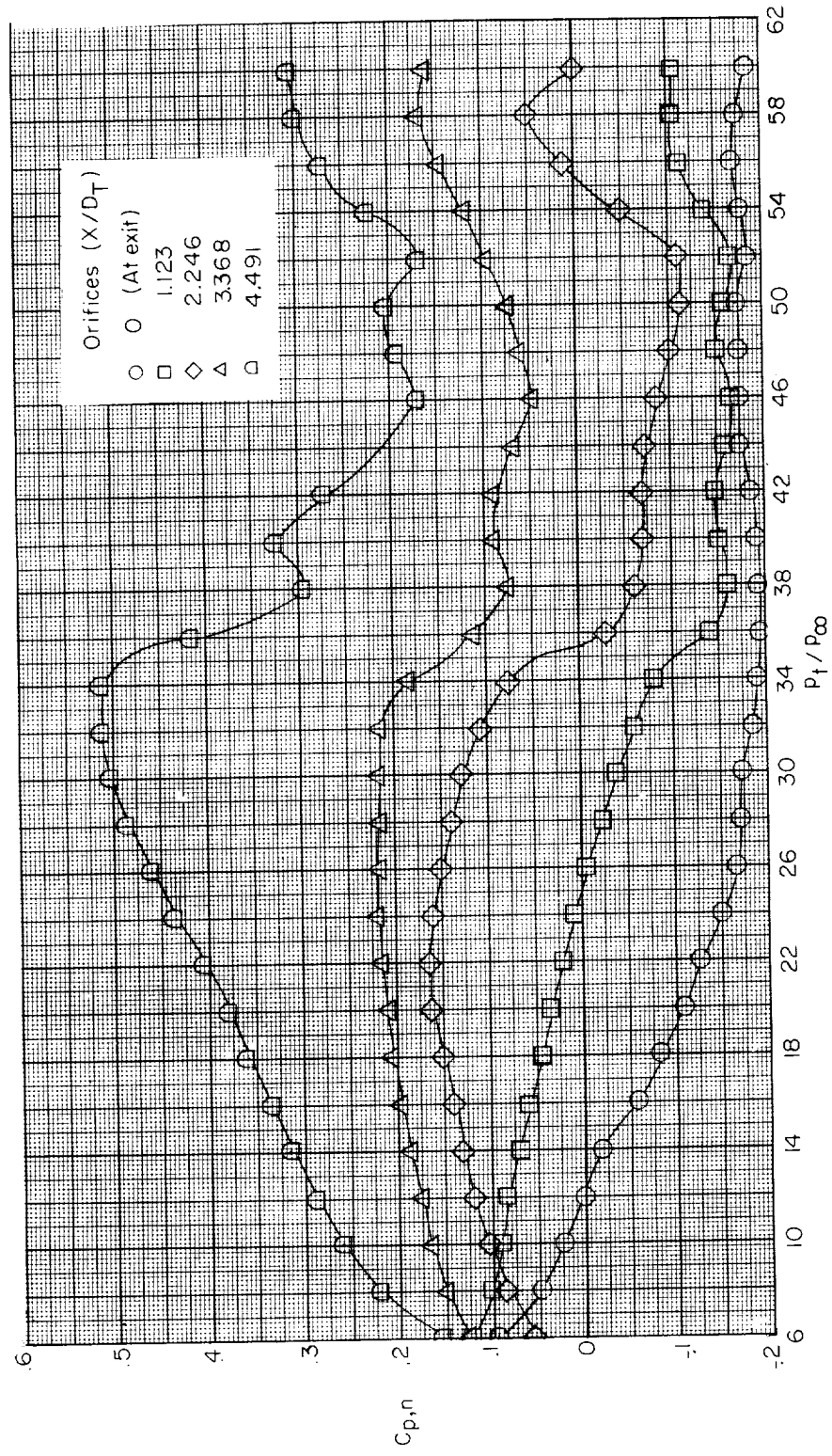
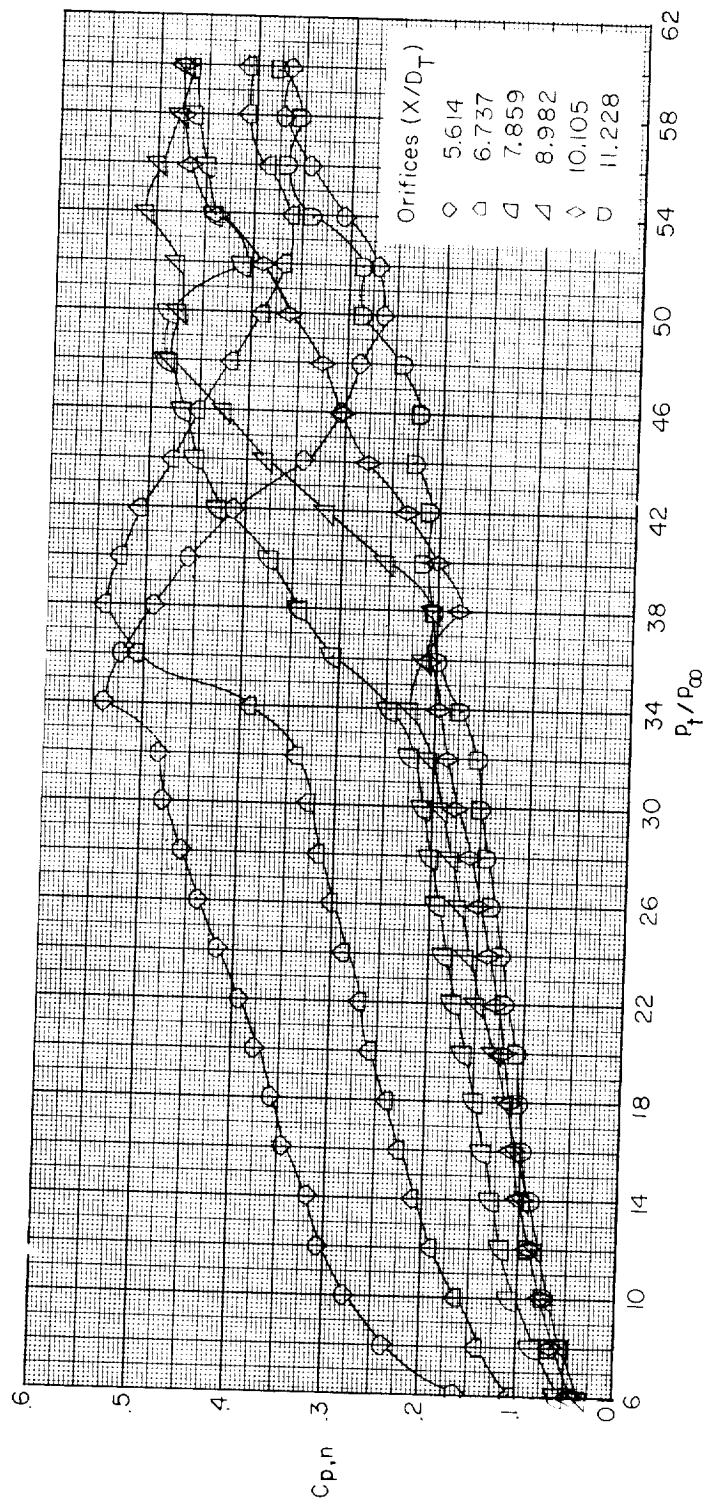
(a) Orifices 2 to 6 ( $x/D_T$ , 0 to 4.491).

Figure 12.- Variation of jet-on pressure coefficient with rocket-exit total-pressure ratio for various orifices located on the rocket center line for test position E.



(b) Orifices 7 to 12 ( $x/D_T$ , 5.614 to 11.228).

Figure 12.- Concluded.

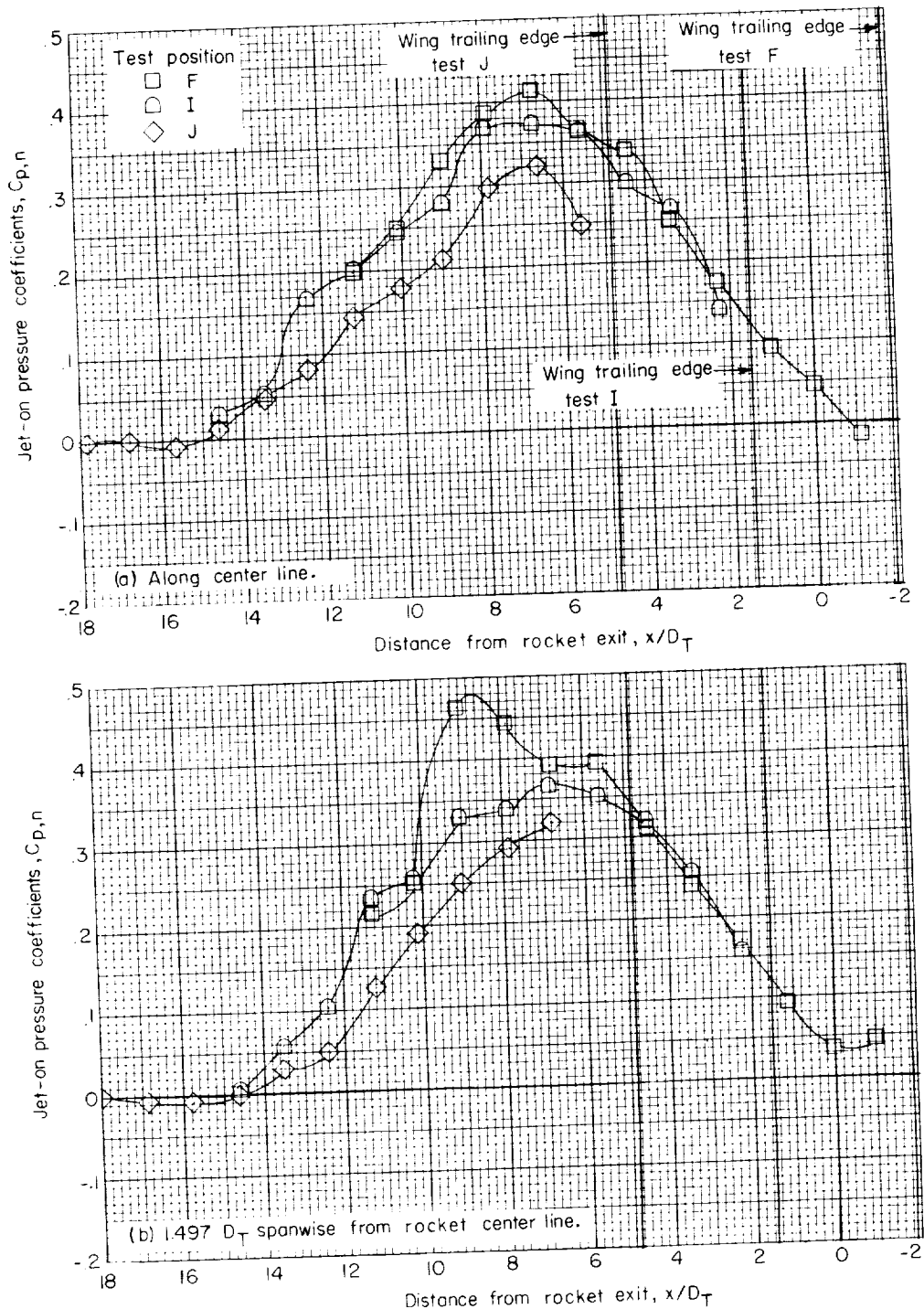


Figure 13.- Chordwise variation of jet-on pressure coefficients at positions F, I, and J for a rocket pressure ratio of 46.

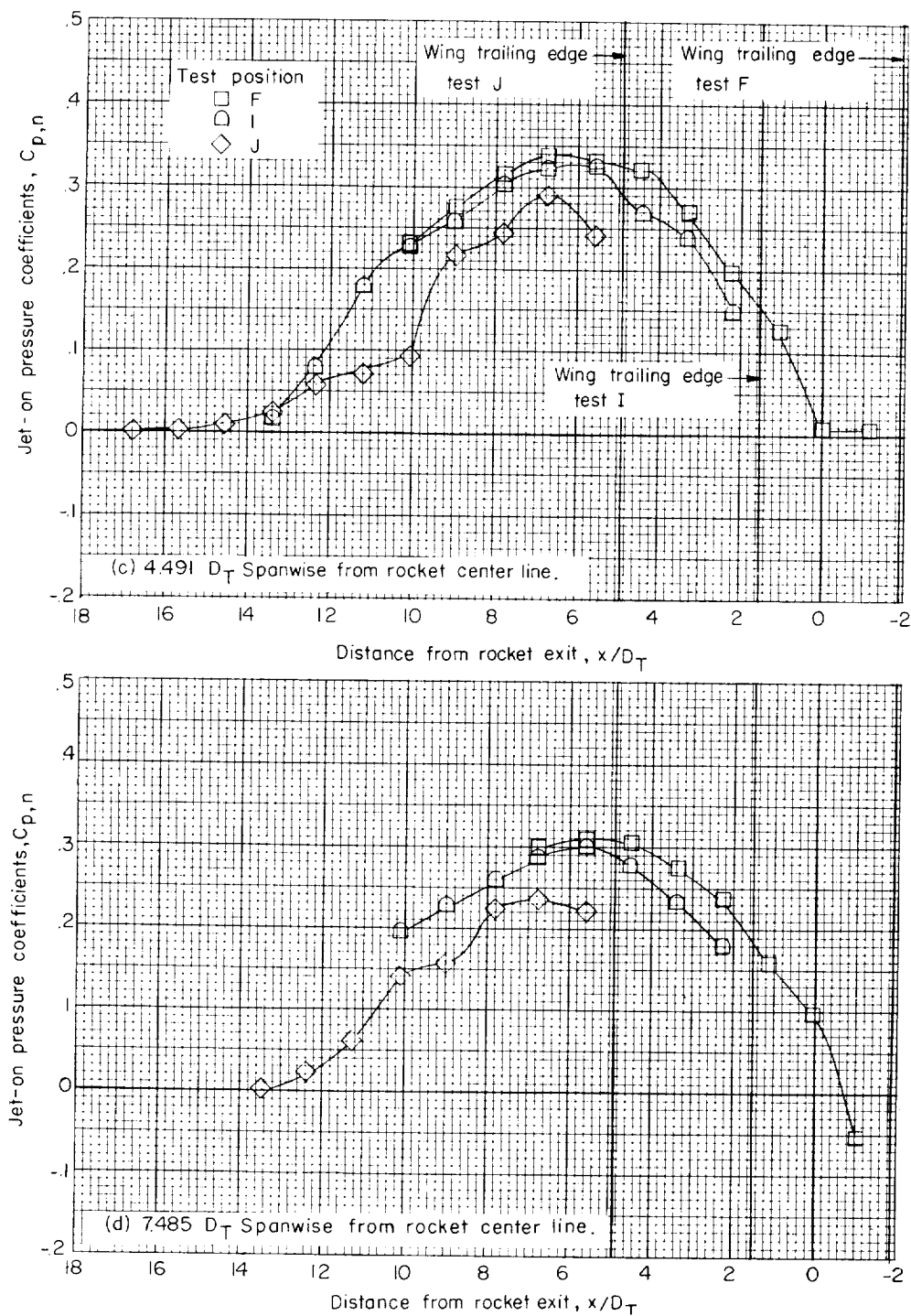


Figure 13.- Concluded.

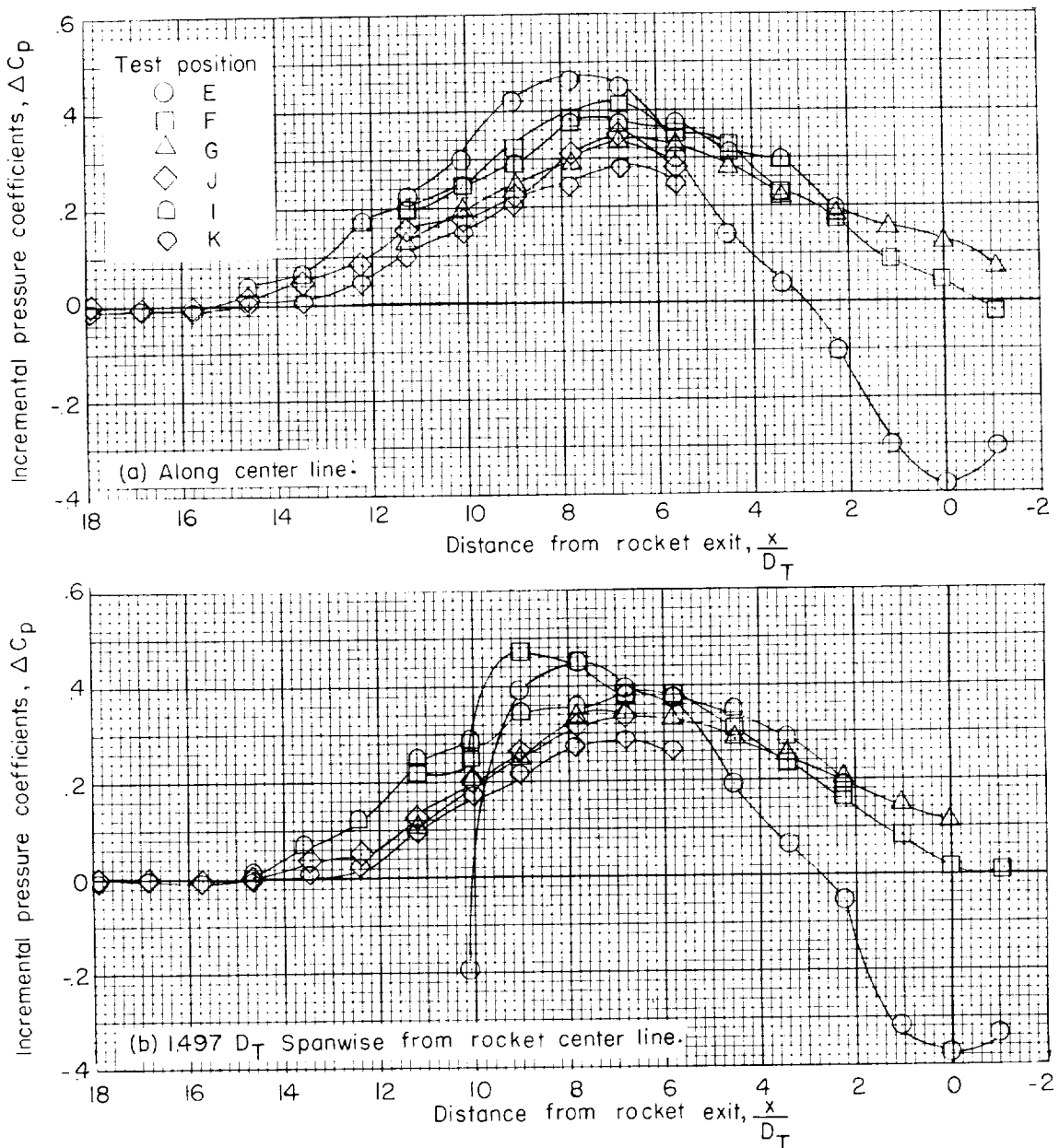


Figure 14.- Chordwise variation of incremental pressure coefficient  $C_{p,n} - C_{p,f}$  at four spanwise stations for positions E, F, G, I, J, and K at a rocket pressure ratio of 46.

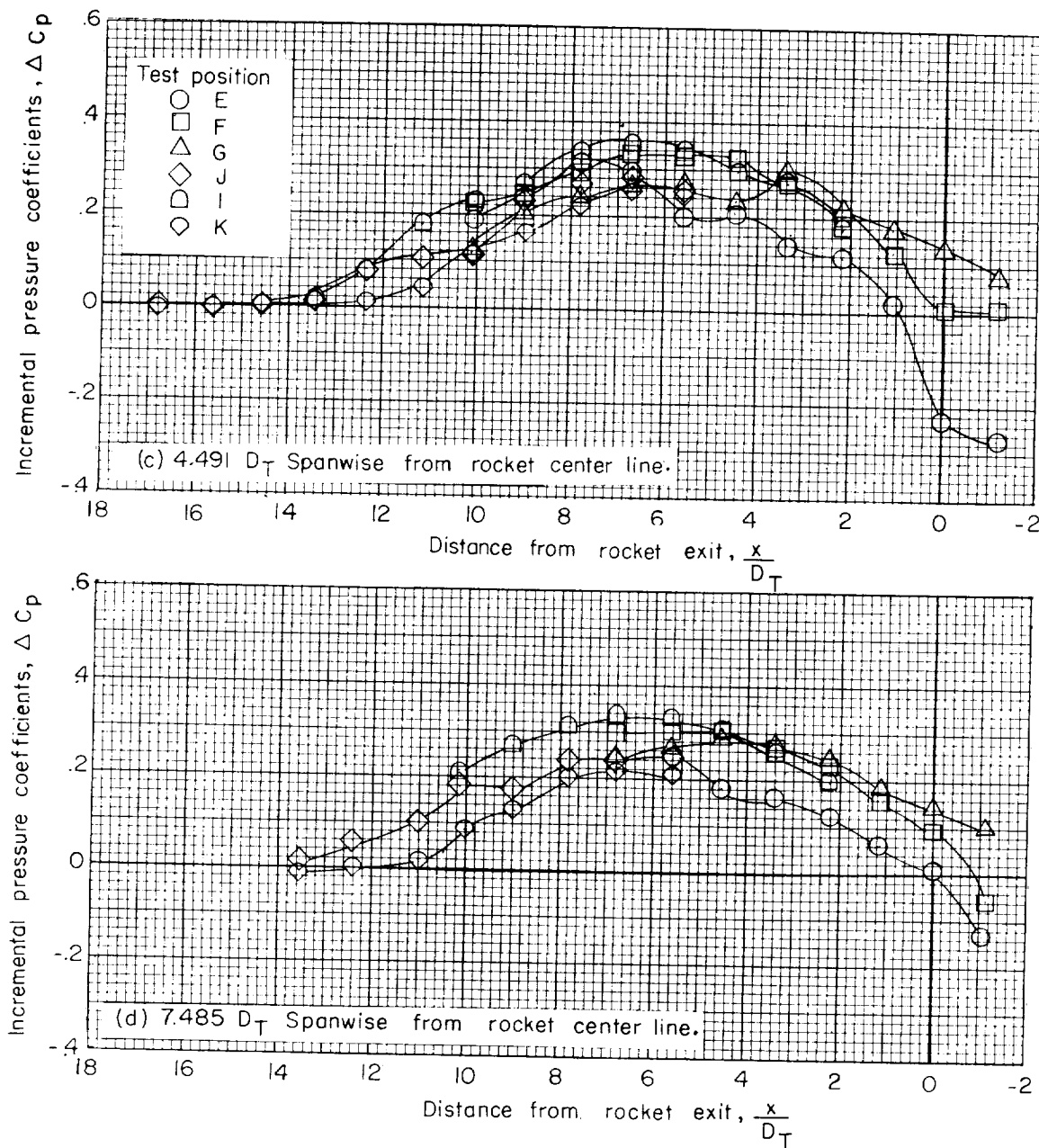


Figure 14.- Concluded.

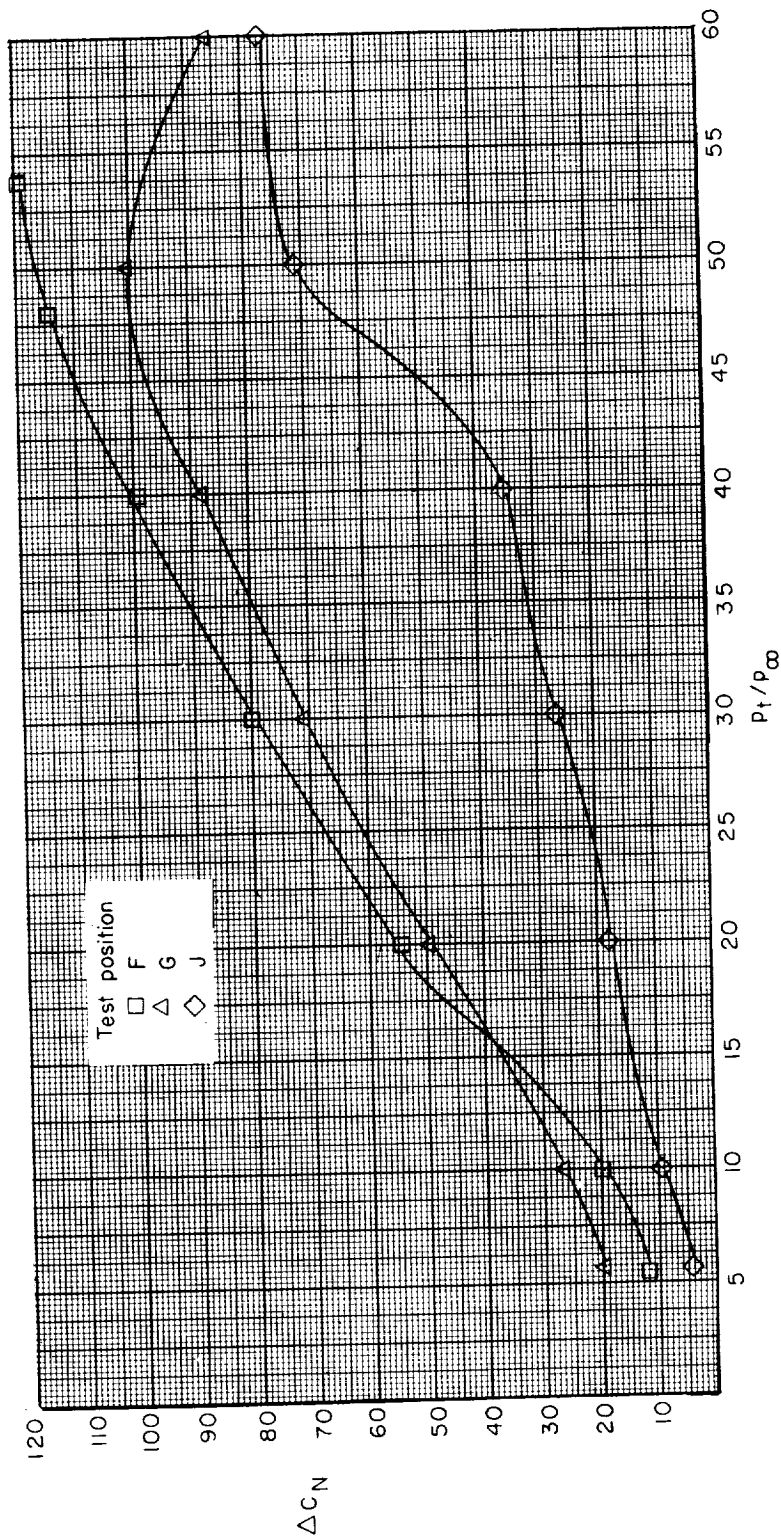


Figure 15.- Variation of incremental normal-force coefficients based on  $A_T$  as a function of rocket total-pressure ratio for test positions F, G, and J.



